Asian Journal of Chemistry; Vol. 32, No. 3 (2020), 706-726

ASIAN JOURNAL OF CHEMISTRY

https://doi.org/10.14233/ajchem.2020.22507

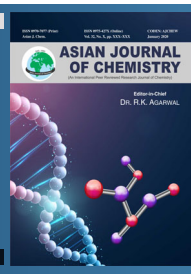

Computational Study of Novel 2,3-*Bis*[(1-methyl-1*H*-imidazole-2-yl)sulfanyl]quinoxaline: Structural Aspects, Spectroscopic Investigation, HOMO-LUMO, MESP, NLO, ADMET Predictions and Molecular Docking Studies as Potential Biotin Carboxylase and Antibiotics Resistant Aminoglycoside Phosphotransferase APH(2'')IVA Enzyme Inhibitor

ASHUTOSH KUMAR*, ANJALI PANDEY and ANIL MISHRA*

Department of Chemistry, Faculty of Science, University of Lucknow, Lucknow-226007, India

*Corresponding authors: E-mail: mishraanil101@hotmail.com; ashutosh.chemist@gmail.com

Received: 19 October 2019; *Accepted*: 11 December 2019; *Published online*: 31 January 2020; AJC-19782

In this paper, a complete quantum chemical calculation has been done to describe the relevant structural aspects of novel 2,3-*bis*[(1-methyl-1*H*-imidazole-2-yl)sulfanyl]quinoxaline with combination of DFT/B3LYP method 6-311++G(d,p) basis set in gas phase and in solvent phase. The molecular structure was examined by using IR, ^{1}H & ^{13}C NMR and UV-visible techniques and solvent effect on spectroscopic properties are also discussed. The vibrational assignments are analyzed by PED using Gauss View 5.0 and VEDA 4.0 program. The ^{1}H NMR and ^{13}C NMR chemical shifts are calculated using the gauge-independent atomic orbital method (GIAO method) in gas phase and in solvents (water, DMSO and chloroform). The UV spectrum is calculated by using TD-DFT/6-311++G(d,p) method in gas phase and in solvent (water, DMSO and chloroform) using IEF-PCM model. With the help of theoretical calculations chemical activities, electrophilic/nucleophilic nature and sites in the molecule, molecular and chemical properties that cannot be obtained by experimental way are obtained. Accordingly, molecular electrostatic potential (MESP), hardness (η)/softness (S) parameters, net charges analyses are investigated to gain electrophilic and nucleophilic nature. Also the sites in molecule and Fukui function analysis are discussed. The dipole moment (μ), polarizability (α_{tot}), anisotropic polarizability ($\Delta\alpha$) and first-order hyperpolarizability (β_{tot}) of the title compound are reported and results shows that the material is capable to generate non-linear effect (NLO). The *in silico* study of all the biological and ADMET properties of title molecule are also discussed and compared with reference drug ciprofloxacin antibiotics. The title molecule and reference drug ciprofloxacin docked with biotin carboxylase enzyme (PDB ID: 2V59) of *E. coli* and aminoglycoside phosphotransferase APH(2")IVA (PDB ID: 4DFU) of *Enterococcus casseliflavus* receptor with the help of Molegro molecular viewer 2.5 program and binding affinity (ΔG) were determined by ParDock server.

Keywords: Quinoxaline, DFT calculations, Spectroscopic properties, Molecular docking, NLO, ADMET.

INTRODUCTION

In the last decades to present, the prominent increase in the number of pathogenic bacteria with substantial resistance to antibiotics has been well documented in the literature [1,2], popular media and books. For example, resistance is particularly problematic in the Gram-positive bacteria enterococcus *e.g.*, vancomycin-resistant enterococcus (VRE) and *Staphylococcus aureus e.g.*, methicillin resistant *Staphylococcus aureus* (MRSA) as well as a number of Gram-negative bacteria like *Acinetobacter baumannii*, *Pseudomonas aeruginosa*, *Klebsiella pneumonia* [3] and *E. coli*. In order to diminish this problem of resistant bacteria, novel antibiotics directed against new target molecules gravely needed. The enzymes of fatty acid biosynthetic pathway are a potential target for the development of novel antibacterial agents [4-6] and the modifying enzyme to help in reducing the resistant power of bacteria because modifications in enzymes results high level of resistance power [7]. The number of aminoglycoside modifying catalyst known the genetic surroundings wherever committal to writing genes square measure settled and therefore the bacterium unable to support accelerator resistance to aminoglycoside. There are three types of aminoglycoside enzymes: (i) N-acetyltransferase (AAC), (ii) O-adenyltransferase (ANT)

and (iii) O-phosphotransferase (APH) [8]. Herein, biotin carboxylase (BC) of *E. coli* (PDB ID: 2V59) and aminoglycoside phosphotransferase APH(2")-ID/APH(2")-IVA (PDB ID: 4DFU, UniProtKB: O68183) of *Enterococcus casseliflavus* are valid as targets for medicament development.

Biotin carboxylase (BCs; EC: 6.3.4.14) (PDB ID: 2V59) represent the subunit of Acetyl-CoA carboxylase of *E. coli* strain K-12. Acetyl-CoA carboxylase enzyme in bacteria composed of three distinct protein units: biotin carboxylase (BCs), biotin carboxyl carrier protein (BCCP) and carboxyltransferase. Acetyl-CoA carboxylase is an enzyme (ACC) that catalyzes the two-step reaction [9]. In the first step, the ATP-dependent carboxylation of the vitamin biotin is catalyzed by biotin carboxylase (BC) enzyme; this is covalently attached to the biotin carboxyl carrier protein (BCCP). In the second step, the transfer of the carboxyl group from biotin to acetyl-CoA to form malonyl-CoA is catalyzed by carboxyltransferase enzyme, which is a substrate for fatty acid synthase. In Gram-negative and Gram-positive bacteria, carboxyltransferase, BCCP and BC are separate proteins that form a complex *in vivo* [10].

The aminoglycoside phosphotransferase APH (2")-ID/APH (2")IVA (PDB ID: 4DFU, UniProtKB: O68183) enzyme of *Enterococcus casseliflavus* are the class of aminoglycoside-modifying enzyme that catalyzes ATP-dependent phosphorylation of hydroxyl group. This activity was proven by the determination of the crystal structure of aminoglycoside enzyme APH (2")-IVA advanced with substance and its antibiotic substrate drug. Herein, we used the novel organic compound 2,3-*bis*[(1-methyl-1*H*-imidazole-2-yl)sulfanyl]quinoxaline as an inhibitor and reference drug ciprofloxacin as an antibiotic for the development of the novel drug to cure the resistant bacterial infections.

Quinoxaline derivatives are biologically active class of nitrogen containing heterocyclic compounds and composed of benzene fused to a pyrazine ring. It is bioisoster of naphthalene, quinoline and benzothiophene which are known leads for many antibiotics [11-14]. An imidazole containing quinoxaline derivatives continuously attracts researcher because of their wide spectrum of biological properties like antivirus [15], antibacterial [16,17], antitubercular [18], antifungal [19], anticancer [20] and neuroprotective [21]. Some quinoxaline containing antibiotics moieties such as actinoleutin, echinomycin and levomycin are among most widely prescribed as antimicrobial drugs.

Screening of new class of drugs using *in vivo* and *in vitro* analysis is becoming increasingly time consuming, difficult and costly due to high number of drugs under investigation. The *in silico* approaches using computational techniques (quantum chemical study, homology modeling, molecular dynamics and docking techniques *etc*.) helping in the drug discovery process by making the analysis cost effective and resource efficient. With help of computational chemistry mechanism and techniques with minimum cost and time more drugs can be discovered. Therefore, the main advantage of *in silico* drug designing approaches is its cost-effectiveness in research and development of drugs. Advantages of using *in silico* approaches can be utilized in all stages of drug development *i.e.* from the preclinical stage to last stage of clinical development. CADD (computer-aided drug design) helps to screen the most potent and important medicinal compound with high efficiency [22]. Therefore molecular docking studies helps in identification of unorthodox small molecular scaffold as well as gives a clear insight, in understanding the properties of any compound such as electron distribution, binding energy, hydrogen bond, donor-acceptors, hydrophobicity and protein-ligand interaction with selectivity/affinity for the target, drug likeness and propose structural hypotheses of how the ligands inhibits the targets, which is invaluable in lead optimization [23]. In this work, the structure of title molecule is fully optimized and characterized by UV/visible, IR and ^{1}H & ^{13}C NMR and a complete comparison between calculated data obtained from DFT method in gas phase and solvent phase (water, DMSO and chloroform) of the title compound. All the theoretical calculations using density functional theory (DFT) method combined with standard 6-311++G(d,p) basis set in the gas phase and solvent phase (water, DMSO and chloroform) using IEF-PCM model have been implemented to search for global chemical reactivity and structural properties of novel 2,3-*bis*[(1-methyl-1*H*-imidazole-2-yl)sulfanyl]quinoxaline that could not be examined by experimental techniques. The electronic properties of novel 2,3-*bis*-[(1-methyl-1*H*-imidazole-2-yl)sulfanyl]quinoxaline were discussed from HOMO-LUMO energies, total density of state (TDOS), ESP, contour map and absorption spectrum were calculated using TD-DFT/B3LYP/6-311++G(d,p) method in gas phase and solvent phase (water, DMSO and chloroform) and ^{1}H and ^{13}C NMR chemical shifts of title molecule were calculated by the GIAO method in gas phase and solvent phase (water, DMSO and chloroform) using IEF-PCM model. The chemical reactivity, local reactivity, electrophilic and nucleophilic attack were also calculated by Fukui function (FF), ESP, MPA and some thermodynamic properties such as entropy, enthalpy and heat capacity at 298.15 K and 1 atm pressure have been calculated to gain deeper insight of the thermo chemistry of the title molecule. The dipole moment, linear polarizability, anisotropy of polarizability and first-order hyperpolarizability values were investigated and the results of these properties were given information about the material capability to generate non-linear optical effects. Non-linear optical active materials have attain awareness with respect to their future possible application in the field of optoelectronics such as optical computing, microchips, optical processing, fiber-optic communication, optical phase conjugation, optical parametric oscillators, optical switching and optical data storage. The interaction of title molecule with biotin carboxylase protein and antibiotic resistance enzyme aminoglycoside phosphotransferase, physicochemical parameter and all the biological properties correlate with the global reactivity parameter such as HOMO, LUMO, HLG (HOMO-LUMO gap), ESP and ΔN_{max}, *etc*.

COMPUTATIONAL METHODS

The quantum chemical calculation of the title molecule have been performed at DFT/B3LYP/6-311++G(d,p) in the gas phase and solvent (water, DMSO and chloroform) using the Gaussian 09 program [24]. In the theoretical calculations the first step is geometry optimization; therefore equilibrium geometry optimization of the title molecule was carried out

by energy minimization method. The molecular structure was drawn by Chemdraw ultra 12.0 [25] and optimized geometry of the title molecule is shown in Fig. 1. The IR intensities and wave numbers (cm^{-1}) calculated at B3LYP/6-311++G(d,p). The vibrational wave number assignments of title molecule were carried out by combining results of the Gauss View 5.0.8 program [26] and VEDA 4 program [27]. The global chemical reactivity descriptors were calculated at DFT in the gas phase and solvent (water, DMSO and chloroform) using IEF-PCM model and shows good agreement and correlate with the biological properties. The local reactivity descriptors such as Fukui function analysis (f_k^+ and f_k^-), local softness (s_k^+ and s_k^-) and local electrophilicity indices (ω_k^- and ω_k^+) were calculated at DFT/6-311++G(d,p) method in the gas phase. The thermodynamic properties of the title molecule were calculated at 298.15 K and 1 atm pressure using DFT/6-311++G(d,p) method in the gas phase. The non-linear optical (NLO) behaviour of the title molecule components of electric moments such as dipole moments (μ_{tot}), polarizability (α_{tot}), anisotropy of polarizability ($\Delta\alpha_{tot}$) and hyperpolarizability (β_{tot}) were calculated using DFT/6-311++G(d,p) method in the gas phase. The nuclear magnetic resonance (NMR) chemical shifts of the title molecule were performed using GIAO (Gauge-Independent Atomic Orbital) method [28,29] at DFT/B3LYP/6-311++G(d,p) in the gas phase (ε = 1.0) and solvent phase {water (ε = 78.35), DMSO (ε = 46.82), chloroform (ε = 4.71)} and the ^1H and ^{13}C isotropic chemical shifts of the title molecule were referenced to the corresponding values of TMS, which was calculated at the B3LYP/6-311+(2d,p) GIAO level of theory. The effect of solvent on the theoretically calculated NMR chemical shifts of the title molecule was included using IEF-PCM model provided by Gaussian 09 Revision-A.02. The frontier molecular orbital (FMO) and electronic absorption spectrum for optimized geometry of title molecule were obtained by TD-DFT (time dependent density functional theory) at B3LYP/6-311++G(d,p) level in gas phase and solvent phase {water (ε = 78.35), DMSO (ε = 46.82), chloroform (ε = 4.71)} by implementing IEF-PCM model available in Gaussian 09 Revision-A.02 and total density of state (TDOS) spectrum of the title molecule was calculated by using Gauss-Sum 2.2 program [30] using TD-DFT output file of Gaussian. The mathematical details used for the calculations of global reactivity descriptors; local reactivity descriptors, non-bonding orbital (NBO) and non-linear optical (NLO) properties have already been reported [31-34].

***in silico* Bioactivity evaluation and pharmacological investigations:** The potential biological activities of title molecule were evaluated from free online server [35]. The physico-chemical properties such as surface tension (γ), index of refraction (n), parachor (Pr) and density (d) of the title molecule were calculated using ACD/Chem Sketch program [36], log $P_{o/w}$, molecular weight, number of hydrogen bond donor, number of hydrogen bond acceptor, number of rotatable bonds, number of heavy atoms, number of aromatic heavy atoms, fraction Csp^3 and GI absorption were evaluated from swissadme free online server [37]. To find out the drug like properties of title molecule, the ADMET (absorption, distribution, metabolism, excretion and toxicity) properties and other physicochemical parameter based on Lipinski rule of five, CMC like rule, MDDR like rule, lead like rule, WDI like rule and bio-availability score of title molecule were evaluated from preADMET server [38]. The solubility parameter (log S) and drug likeness score were determined from Molsoft L.L.C. free online server [39]. The oral toxicity of title molecule in term of LD_{50} was checked using ProTox server [40].

Molecular docking study

Ligand input file and protein preparation for docking: The molecular structure of title molecule was drawn and optimized by using GaussView 5.0 program package. The optimized structure of title molecule was used to analyze the molecular docking studies also. The 3-D structure of biotin carboxylase 2.4 Å (PDB ID: 2V59) and the structure of antibiotic resistance enzyme aminoglycoside phosphotransferase 1.98 Å (PDB ID: 4DFU) were obtained from protein data bank (PDB) [41]. Moreover, the structure of molecule was used from 3-D structure (gjf file format) by converting the gjf file into the mol file. The PDB file of protein was imported without removing water molecule, hydrogen and removed only the external ligands of proteins. The protein-ligand docking study was performed and results were analyzed by using molegro molecular viewer (MMV) version 2.5.0 [42] and ParDock (automated server for protein-ligand docking and used for energy minimization of docked structure and protein-ligand binding free energy estimations) [43].

RESULTS AND DISCUSSION

Molecular geometry and structural properties: The novel 2,3-*bis*[(1-methyl-1*H*-imidazole-2-yl)sulfanyl]quinoxaline

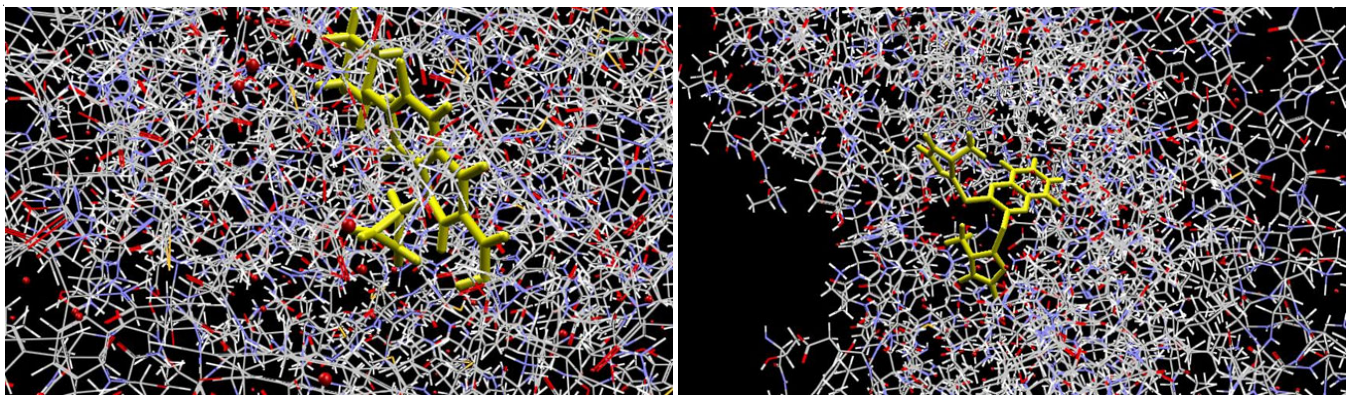

Fig. 1. Docked structure of title molecule with protein 2V59 and 4DFU

molecule is a substituted quinoxaline with two sulfanyl groups and two imidazole rings with methyl group that planer quinoxaline ring. The optimized geometry of the title molecule was performed by B3LYP/6-311++G(d,p) in gas phase methods with atoms numbering and symbol (Fig. 2). The selected and comparative optimized geometrical parameters such as bond length, bond angle values are listed in Table-1 and dihedral angle values are listed in Table-2. The slightly change in bond lengths, bond angles and dihedral angels due to the electron donating groups and electron withdrawing groups affects the electron density on the ring carbon atoms. The actual change in the C-H bond lengths would be influenced by the combined effects of the inductive–mesomeric interactions and the electric dipole field of the polar substituent like sulfanyl groups of title molecule. The bond lengths of C-C bond are differing in values, which is due to the substitutions on the quinoxaline ring in the place of hydrogen atom. The optimized sulfanyl groups (-S-) on C1 and C4 carbon atoms, C1-S15 bond length is 1.7954 Å and C4-S16 bond length is 1.7954 Å in DFT level of theory. The bond lengths of quinoxaline ring such as C1-N13, C2-N13, C3-N14 and C4-N14 bonds are 1.3003, 1.3666, 1.3666 and 1.3003 Å at DFT level, respectively. The C17-N27, C17-N28, C22-N29 and C22-N30 bond lengths in the imidazole ring at DFT level of theory are 1.3174, 1.3737, 1.3737 and 1.3174 Å, respectively. Table-1 showed that the bond angle in quinoxaline ring around S15 and S16 [C4-C1-S15 = 118.35, N13-C1-S15 = 120.33°, C1-C4-S16 = 118.35° and N14-C4-S16 = 120.33° at DFT level] indicates the less difference in the bond angles. In the imidazole ring nitrogen atoms substituted by methyl groups makes the angle C17-N28-C35, C19-N28-C35, C24-N29-C31 and C22-N29-C31 as greater 127.72°, 126.01°, 126.02° and 127.71° at DFT level of theory, respec-

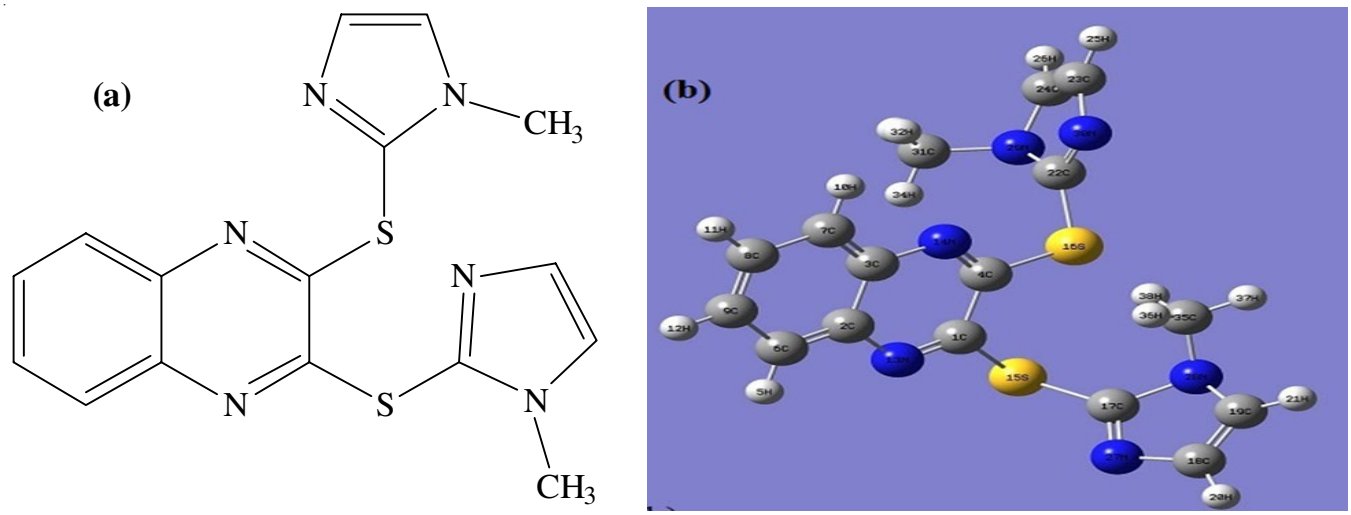

Fig. 2. (a) Chemical structure of 2,3-*bis*[(1-methyl-1*H*-imidazole-2-yl)sulfanyl]quinoxaline and (b) the optimized structure of title molecule at B3LYP/6-311++G(d,p) level

TABLE-1
BOND LENGTH AND SELECTED BOND ANGLE OF NOVEL 2,3-*BIS*[(1-METHYL-1*H*-IMIDAZOL-2-YL)SULFANYL]QUINOXALINE USING DFT/6-311++G(d,p) LEVEL OF THEORY IN THE GAS PHASE

Parameters	Bond length (Å)	Parameters	Bond length (Å)	Parameters	Bond angle (°)	Parameters	Bond angle (°)
C1-C4	1.4500	C18-H20	1.0788	C4-C1-N13	121.309	C24-N29-C31	126.02
C1-N13	1.3003	C18-N27	1.3683	C4-C1-S15	118.356	C22-N29-C31	127.71
C1-S15	1.7954	C19-H21	1.0779	N13-C1-S15	120.334	C17-N28-C35	127.72
C2-C3	1.4223	C19-N28	1.3737	C3-C2-N13	120.307	C19-N28-C35	126.01
C2-C6	1.4126	C22-N29	1.3737	C6-C2-N13	120.116	C17-N28-C19	106.06
C2-N13	1.3666	C22-N30	1.3174	C2-C3-N14	120.305	C17-N27-C18	105.37
C3-N14	1.3666	C23-C24	1.3742	C7-C3-N14	120.116	N28-C35-H36	110.57
C4-N14	1.3003	C23-H25	1.0788	C1-C4-N14	121.31	N29-C31-H34	109.38
C4-S16	1.7954	C23-N30	1.3683	C1-C4-S16	118.352	H32-C31-C33	109.75
H5-C6	1.0835	C24-H26	1.0779	N14-C4-S16	120.33	H32-C31-C34	109.05
C6-C9	1.3777	C24-N29	1.3737	C1-S15-C17	101.64	C33-C31-H34	109.02
C7-C8	1.3777	N28-C35	1.4563	C4-S16-C22	101.65	N28-C35-H38	109.38
C7-^{1}H0	1.0835	N29-C31	1.4563	C3-C2-C6	119.57	H36-C35-H37	109.57
C8-C9	1.4134	C31-H32	1.0918	S15-C17-N27	124.02	H36-C35-H38	109.05
C8-^{1}H1	1.084	C31-C33	1.0899	N27-C17-N28	112.06	H37-C35-H38	109.02
C9-^{1}H2	1.084	C31-C34	1.0893	C19-C18-N27	110.32	N29-C31-H32	110.57
S15-C17	1.7642	C35-H36	1.0918	C18-C19-N28	106.15	N29-C31-C33	109.02
S16-C22	1.7642	C35-H37	1.0899	S16-C22-N29	123.72	H26-C24-N29	121.71
C17-N27	1.3174	C35-H38	1.0893	S16-C22-N30	124.02	C22-N30-C23	105.33
C17-N28	1.3737	C3-C7	1.4126	N29-C22-N30	112.06	C22-N29-C24	106.06
C18-C19	1.3742	–	–	C24-C23-N30	110.32	S15-C17-N28	123.71
				C23-C24-N29	106.15	–	–

TABLE-2
DIHEDRAL ANGLE (°) OF NOVEL 2,3-*BIS*[(1-METHYL-1*H*-IMIDAZOL-2-YL)SULFANYL]QUINOXALINE USING DFT/6-311++G(d,p) LEVEL OF THEORY IN THE GAS PHASE

Parameters	Dihedral angle (°)	Parameters	Dihedral angle (°)	Parameters	Dihedral angle (°)
N13-C1-C4-N14	-1.0318	C1-S15-C17-N27	104.3624	S15-C17-N28-C35	8.5203
N13-C1-C4-S16	179.0981	C1-S15-C17-N28	-81.119	N27-C17-N28-C35	-176.38
S15-C1-C4-S16	-0.7733	C4-S16-C22-N29	-81.132	C19-N28-C35-H36	-89.3326
C4-C1-N13-C2	0.7974	C4-S16-C22-N30	104.3499	C19-N28-C35-H38	150.5547
S15-C1-N13-C2	-179.3337	S15-C17-N28-C19	-176.4271	C22-N29-C31-H32	84.7621
C6-C2-C3-N14	-179.7241	N27-C18-C19-N28	-0.3555	C22-N29-C31-H33	-154.4813
N13-C2-C3-C7	-179.7227	C18-C19-N28-C35	176.2539	C24-N29-C31-H32	-89.3599
N13-C2-C3-N14	0.2325	S16-C22-N29-C31	8.52	C24-N29-C31-H33	31.3968
S16-C4-N14-C3	-179.3323	S16-C22-N29-C24	-176.4248	C24-N29-C31-H34	150.5272
C1-C4-S16-C22	-172.6555	N30-C22-N29-C31	-176.3112	H26-C24-N29-C22	-179.1066
N14-C4-S16-C22	7.473	N29-C22-N30-C23	0.9746	–	–

tively in the imidazole ring. In the quanoxaline ring, the nitrogen atom is slightly out-of-plane, with a torsional angle N13-C1-C4-N14 in the -1.0318°, S15-C1-C4-S16 in the -0.7733°, N13-C2-C3-N14 in the 0.2325° at DFT level of theory in the gas phase. From Tables 1 and 2, the comparative analysis of geometric data of title molecule indicates that the intermolecular hydrogen bonding affect the geometric parameter, particularly the N and S atoms of the title molecule. From the geometric data, it is clear that the title molecule act as good ligand for pharmaceutical industries.

Global reactivity descriptors: Frontier molecular orbitals (FMOs) play an important role in the study of optical and electronic properties, UV-visible spectra, as well as in the quantum chemistry [44]. Molecular orbitals (MO) play an important role in quantum chemistry for the understanding of the chemical reactivity at the atomic level and chemical reactions. HOMO (highest occupied molecular orbital) and LUMO (lowest unoccupied molecular orbital) are named as FMOs. HOMO consider as electron donor and LUMO consider as electron acceptor. HOMO energy is directly related to electron donating power, more is the HOMO energy more will be electron donating power. The energy gap between HOMO and LUMO deduces the chemical reactivity, kinetic stability, optical polarizability and hardness and softness of the molecule [44-46]. The hard molecule or atoms are not more polarizable than the soft ones because they need more energy to excitation. According to Mabkhot *et al.* [47], HOMO-LUMO gap (ΔE_{gap}) is an established parameter to measure the extent of the intramolecular charge transfer between ligand and protein (enzyme) and was used in pharmaceutical studies. The electrophilicity index (ω) can be deduces the flow of electrons between donor and acceptor [47]. A more reactive and strong electrophiles is identified by a high value of electrophilicity index (ω) and chemical potential (μ); in the molecule escaping tendency of electrons defined by chemical potential (μ). Generally, hard and soft molecule has large energy gap and small energy gap (ΔE_{gap}), respectively (Table-3) and is more reactive in nature [48].

In this paper, the energetic behaviour of the title molecule is evaluated. We carried out all the calculations in the gas phase, water, DMSO and in chloroform solvent using IEF-PCM model at DFT/6-311++G(d,p) level of theory. All the global chemical reactivity descriptors were calculated and listed in Table-3 by using HOMO and LUMO energy values. The ionization potential (I) is defined as $I = -E_{HOMO}$ and electron affinity (A) is defined by $A = -E_{LUMO}$, respectively. The HOMO, LUMO and ΔE_{Gap} energies of the title molecule in gas phase, water, DMSO and chloroform solvent at DFT/6-311++G(d,p) level of theory are -6.63396 eV, -6.80213 eV, -6.79913 eV and -6.74226 eV and -2.98446 eV, -3.10582 eV, -3.10310 eV and-3.05412 eV and 3.64949 eV, 3.69630 eV, 3.69602 eV and 3.68813 eV,

TABLE-3
CALCULATED ENERGY VALUES OF THE TITLE MOLECULE BY DFT/B3LYP/6-311++G(d,p) METHOD IN GAS PHASE AND SOLVENT (WATER, DMSO, CHLOROFORM)

Parameters	Gas phase	Water	DMSO	Chloroform
Ground state energy (Hartree)	-1743.0714	-1743.092	-1743.093	-1743.0855
E_{HOMO} (eV)	-6.63396	-6.80213	-6.79913	-6.74226
E_{LUMO} (eV)	-2.98446	-3.10582	-3.10310	-3.05412
ΔE_{gap}(eV)	3.64949	3.69630	3.69602	3.68813
Ionization potential (IP) (eV)	6.63396	6.80213	6.79913	6.74226
Electron Afinity (EA) (eV)	2.98446	3.10582	3.10310	3.05412
Global hardness (η) (eV)	1.82474	1.84815	1.84801	1.84406
Electronegativity (χ) (eV)	4.80921	4.95398	4.95112	4.89819
Chemical Potential (μ) (eV)	-4.80921	-4.95398	-4.95112	-4.89819
Global softness (S) (eV^{-1})	0.274010	0.270540	0.541121	0.542279
Electrophilicity index (ω) (eV)	6.33746	6.63958	6.632419	6.50527
Electron donating power (ω^-) (eV)	8.97017	5.228730	9.338982	5.170679
Electron accepting power (ω^+) (eV)	4.16095	2.457651	4.387860	2.413196
Net electrophilicity ($\omega^\pm$) (eV)	13.13112	7.6863816	13.726848	7.583876
Dipole moment (Debye)	4.7258	6.3391	6.3139	5.8310
Q^{Max}	2.63555	2.68050	2.67915	2.65619

respectively. Comparative analysis of results of HOMO, LUMO and ΔE gap energies in solvent phase are higher than in gas phase at DFT level and HOMO energy are greater in water solvent. The calculation of chemical hardness (η), electronegativity (χ), chemical potential (μ), global softness (S), electrophilicity index (ω), electron donating power (ω^-), electron accepting power (ω^+), net electrophilicity index ($\omega^\pm$) and maximum amount of electronic charge that an electrophile may accept (Q^{Max}) [49] are based on a finite difference method and thus:

$$\text{Chemical hardness } (\eta) = \frac{(I - A)}{2} \quad (1)$$

$$\text{Electronegativity } (\chi) = \frac{(I + A)}{2} \quad (2)$$

$$\text{Chemical potential } (\mu) = -\frac{(I + A)}{2} \quad (3)$$

$$\text{Global softness } (S) = \frac{1}{2\eta} \quad (4)$$

$$\text{Electrophilicity index } (\omega) = \frac{\mu^2}{2\eta} \quad (5)$$

$$\text{Electron donating power } (\omega^-) = \frac{(3I + A)^2}{16(I - A)} \quad (6)$$

$$\text{Electron accepting power } (\omega^+) = \frac{(I + 3A)^2}{16(I - A)} \quad (7)$$

$$\text{Net electrophilicity } (\omega^\pm) = \omega^+ + \omega^- \quad (8)$$

$$Q^{Max} = -\frac{\mu}{\eta} \quad (9)$$

According to global chemical reactivity descriptors results (Table-3), the simulated FMOs of the title molecule (Fig. 3) indicates the presence of intramolecular charge transfer (ICT) within the molecule. The band gap energy as 3.64949, 3.69630, 3.69602 and 3.68813 eV in gas phase, water, DMSO and chloroform at DFT level, respectively, which confirms that the title molecule has stable structure and the band gap energy values was comparable to the band gap energy values of the bioactive molecules [50] in different solvents and methods. The ionization potential (IP) values in different solvents and gas phase at DFT level indicates that the energy values (6.3396, 6.80213, 6.79913 and 6.74226 eV in the gas phase, water, DMSO and chloroform at DFT level of theory, respectively) is required to remove an electron from the HOMO. From Table-3, a lower value of electron affinity (EA) values indicates that the title molecule readily accepts electrons to form bonds; this indicates the higher molecular reactivity with nucleophiles. The higher hardness and lower softness values of the title molecule confirm the higher molecular hardness associated with the molecule. The lower chemical potential and higher electrophilicity index values identified are comparable with that of the bioactive molecules [51]. The direction of charge transfer is determined by Q^{max} define the maximum amount of electron accepts by electrophiles from the environment. Fig. 4

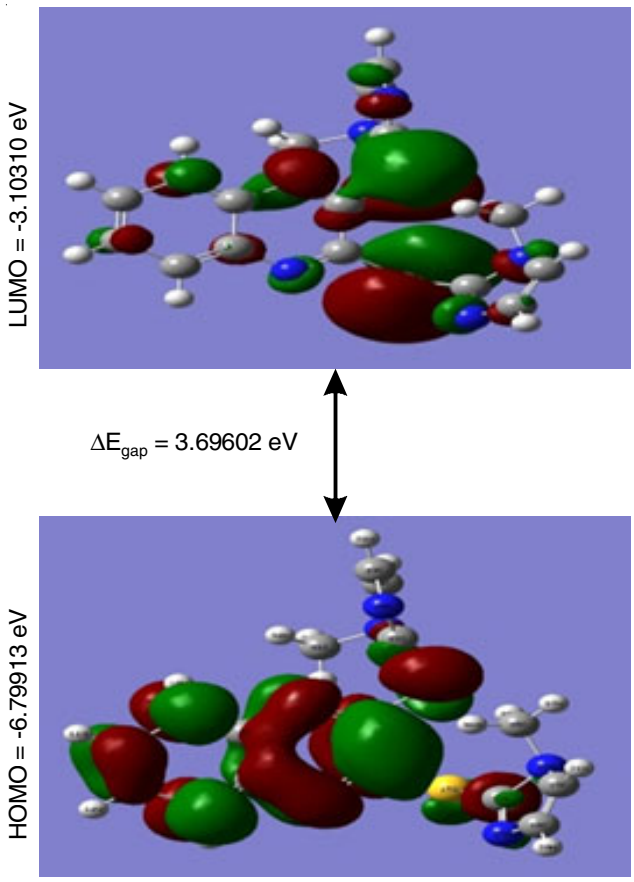

Fig. 3. HOMO-LUMO energy diagram of title molecule (in DMSO solvent)

shows the chemical reactivity parameters deviations in DFT method in gas phase and solvent.

Electronic properties and UV-visible studies: The time dependent-density functional theory (TD-DFT) methods used to understand electronic transitions of organic compounds as well as inorganic compounds. The ultra violet spectra of fully optimized ground state structure of title molecule were investigated by using TD-DFT/6-311++G(d,p) in the water, DMSO, chloroform using IEF-PCM model and correlate with gas phase using same level of calculations have been used to determine the low-lying excited state of title molecule. The theoretical calculations of absorption wavelength (λ_{max}), electronic excitation energy (E), oscillator strengths (f) and major contributions of FMOs are also given in Table-4. Calculations of the molecular orbital geometry show that the absorption maxima of this molecule correspond to the transition between FMOs such as translation from HOMO (MO-85) to LUMO (MO-93) and this transition is assigned as $\pi \rightarrow \pi^*$. The HOMO value -6.63396 eV in the gas phase is distributed over the entire molecule whereas LUMO of the title molecule lies largely over the quinoxaline as well as imidazole ring slightly over the rest of the molecule except the S and N atoms. As can be seen from Table-4, the theoretically calculated absorption maxima values of first three excited states have been found to be 414.15 (f = 0.0093), 403.12 (f = 0.0218), 365.90 nm (f = 0.001750) in water, 414.42 (f = 0.0099), 403.52 (f = 0.0230), 366.04 nm (f = 0.0190) in DMSO, 417.65 (f = 0.0073), 407.48 (f = 0.0212), 366.91 nm (f = 0.0257) in $CHCl_3$ and 425.44 (f = 0.0026), 417.68 (f = 0.0088), 370.12 nm (f = 0.0212) in the gas phase

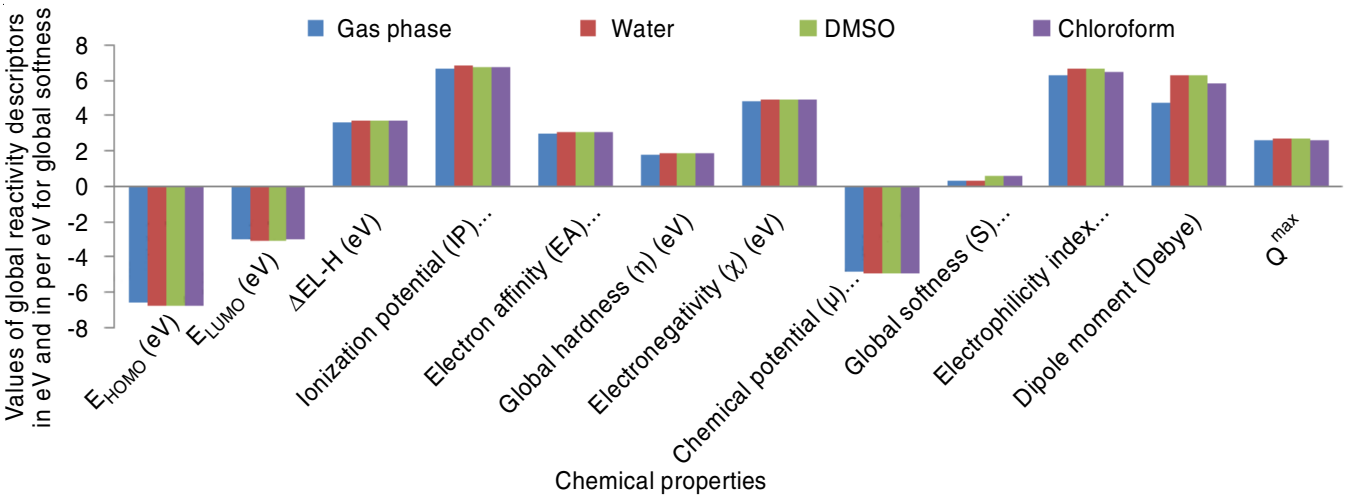

Fig. 4. Global reactivity descriptors parameters plot of the title molecule

TABLE-4
THEORETICAL ABSORPTION WAVELENGTH (λ_{max}), EXCITATION ENERGY (E) AND OSCILLATOR STRENGTHS (f) FOR TITLE MOLECULE CALCULATED AT DFT/B3LYP/6-311++G(d,p) IN THE GAS PHASE AND SOLVENT PHASE (WATER, DMSO AND CHLOROFORM)

λ_{max} (nm)	E (eV)	Oscillator strength (f)	Major contributions (HOMO = H, LUMO = L)	Excitation
Water				
414.15	2.9937	0.0093	H-1→L (36 %), H→L (49 %)	ES-1
403.12	3.0756	0.0218	H-1→L (38 %), H→L (44 %)	ES-2
365.90	3.3885	0.0175	H-2→L (95 %)	ES-3
DMSO				
414.42	2.9917	0.0099	H-1→L (35 %), H→L (50 %)	ES-1
403.52	3.0726	0.0230	H-1→L (39 %), H→L (44 %)	ES-2
366.04	3.3872	0.0190	H-2→L (95 %)	ES-3
Chloroform				
417.65	2.9686	0.0073	H-1→L (40 %), H→L (49 %)	ES-1
407.48	3.0427	0.0212	H-3→L (11 %), H-1→L (34 %), H→L (49 %)	ES-2
366.91	3.3792	0.0257	H-2→L (92 %), H-3→L (4 %)	ES-3
Gas phase				
425.44	2.9143	0.0026	H-1→L (45 %), H→L (36 %)	ES-1
417.68	2.9684	0.0088	H-3→L (10 %), H-1→L (29 %), H→L (55 %)	ES-2
370.12	3.3499	0.0212	H-2→L (84 %), H-3→L (3 %), H-1→L (9 %)	ES-3

at TD-DFT/6-311+G(d,p) method. It is seen from Table-4, calculations performed at water, DMSO and chloroform are close to each other when compared with gas phase and also absorption maxima values of gas phase are larger than that of the solvents phase. The simulated UV absorption spectra of the title molecule are shown in Fig. 5. The character of the FMOs (HOMO & LUMO) and prepare the density of states (DOS) was calculated by using Gauss-Sum 2.2 Program [30]. The density of states (DOS) plot of the title molecule is shown in Fig. 6, the molecular orbital in certain energy range and population analysis per orbital of any molecule was analyzed using the DOS method.

Electrostatic potential (ESP), total electron density (ED) and 2-D contour map plot: In the present study, a three dimensional molecular electrostatic potential (MESP), electrostatic potential (ESP), electron density (ED) and 2-D contour map was obtained from optimized structure and carried out by using B3LYP/6-311++G(d,p) basis set in the gas phase,

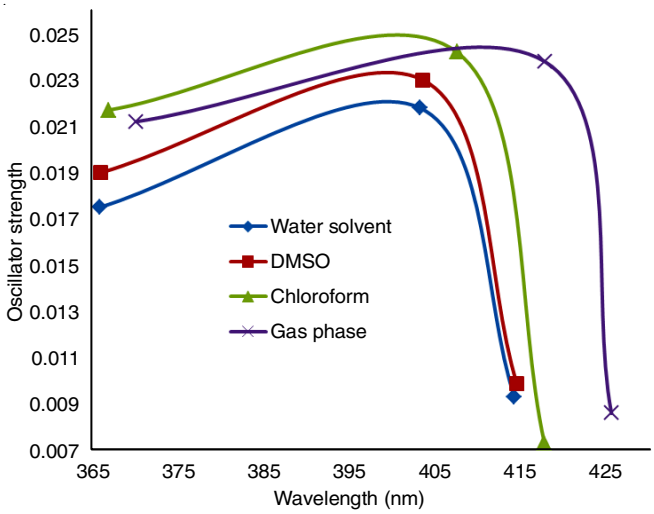

Fig. 5. Simulated UV-visible spectrum of the title molecule in the gas phase and solvent phase

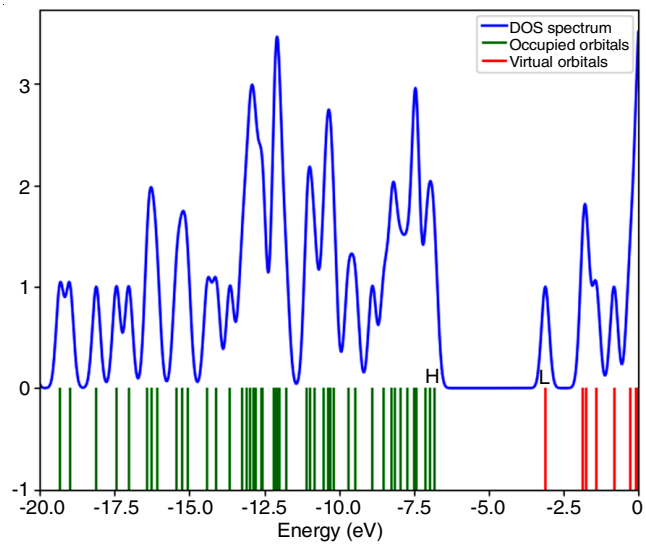

Fig. 6. Total density of state (DOS) spectrum plot of the title molecule

all the maps of the title molecule are illustrated in Fig. 7. The MESP surface map illustrates the electron density allocation over the molecules. It is very useful descriptor in determining sites for nucleophilic and electrophilic as well as hydrogen bonding interactions [52,53]. MESP mapping is very useful in the study of drugs like a molecule with its neighboring environment [54] and physico-chemical property relationships of molecules [55]. The values of the molecular electrostatic potential at MESP delineate by totally different colours like red, blue and inexperienced represent the regions of a lot of negative, a lot of positive and 0 static potentials, severally. Fig. 7 showed that the most negative regions (-0.107e0 a.u.) (red) over the N and S atoms and the most positive region (+0.107e0 a.u.) (blue) over the hydrogen atoms and green colour represents the neutral region in the molecule. The negative and positive regions of the electrostatic potential of title molecule are associated with the electrophilic and nucleophilic reactivity regions in the molecule. This type of active sites found in the molecule is good evidence of biological activity in the title molecule. The 2-D MESP contour map plotted in Fig. 7 provides complete information about the molecular electrostatic potential (distribution) active area, by showing the closer curved lines over the molecule revels maximum values of positive potential and negative potentials corresponding to the electrophilic and nucleophilic regions in the title molecule in the range of +0.107e0 a.u. and -0.107e0 a.u. are occur (at B3LYP functional level), respectively. These regions present in the molecule are more biologically active and shows high molecular interactions.

Local reactivity descriptors: Fukui function analysis (FF): The global properties like chemical potential (μ), hardness (η), softness (S) and electrophilicity index (ω) related to the chemical reactivity, whereas local reactivity is related to the selectivity concept. The Fukui function is the most important local reactivity descriptor parameter. Fukui function indicates the derivatives of electron density with respect to change of number of electrons or it indicates the tendency of the electronic density to impair at a given site upon accepting and donating electrons [56,57] and in other words, it gives the information about highly electrophilic and nucleophilic sites in the mole-

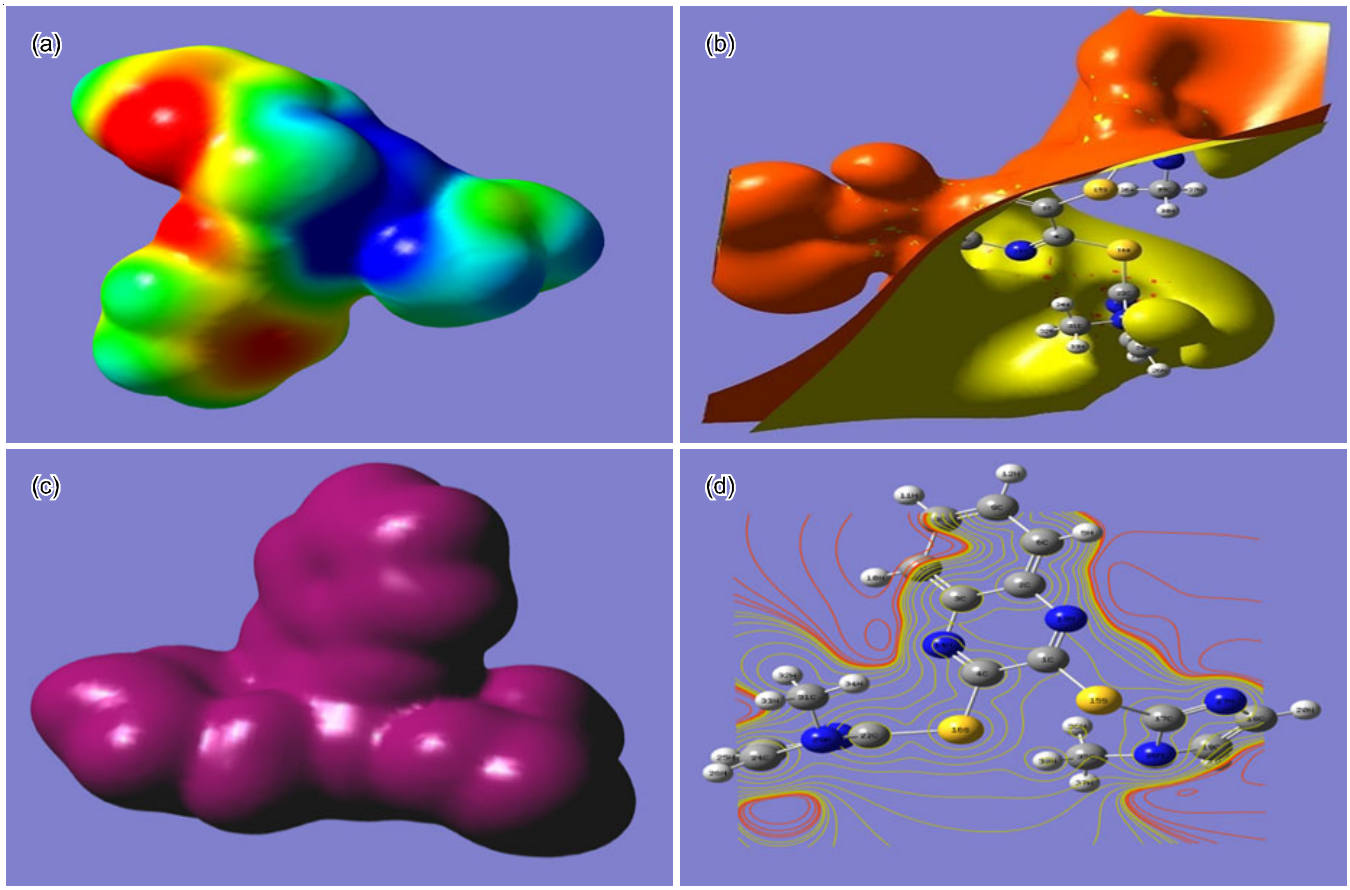

Fig. 7. (a) 3D MESP surface, (b) 3D ESP surface map, (c) electron density (ED) plot and (d) 2D contour map of the title molecule

cule. In practice the best way of calculation of the Fukui functions at atomic resolution is to use the condensed Fukui functions [58] on the kth atom site, for nucleophilic (f_k^+), electrophilic (f_k^-) and free radical (f_k^0) attacks can be expressed as:

For nucleophilic attacks:

$$f_k^+ (r) = q_k (r) (N + 1) - q_k (r) (N) \quad (10)$$

For electrophilic attacks:

$$f_k^- (r) = q_k (r) (N) - q_k (r) (N - 1) \quad (11)$$

For free radical attacks:

$$f_k^0 (r) = q_k (r) (N + 1) - q_k (r) (N - 1) \quad (12)$$

In the above equations, q_k is the atomic charge (evaluated from Mulliken, NPA, Hirshfeld or NBO *etc*.) at kth atomic site in the cationic (N-1), anionic (N+1) or neutral molecule (N). Roy *et al.* [59] proposed the "relative nucleophilicity" (S_k^-/S_k^+) and the "relative electrophilicity" (S_k^+/S_k^-) descriptor for *k*th atoms and this indicates preferred nucleophilic and electrophilic reactive sites for the study of the intermolecular reactivity in the chemical compounds. The nucleophilic and the electrophilic local softness s_k^- and s_k^+ [57] equations are given below:

Nucleophilic local softness:

$$s_k^- = S f_k^- \quad (13)$$

Electrophilic local softness:

$$s_k^+ = S f_k^+ \quad (14)$$

In the above equation S is the chemical softness and f_k^- and f_k^+ are the nucleophilic and electrophilic Fukui functions. Chattaraj *et al.* [60] proposed the concept of generalized philicity ω_k^x (x = –, + or 0) indices to identify the most nucleophilic, electrophilic and radical sites in reactivity and regioselectivity studies of chemical compounds. The local (or condensed) nucleophilicity ω_k^- and electrophilicity ω_k^+ indices are related to the Parr global electrophilicity index (ω) and the corresponding Fukui functions by eqns. 15 and 16 are given below:

Local nucleophilicity:

$$\omega_k^- = \omega f_k^- \quad (15)$$

Local electrophilicity:

$$\omega_k^+ = \omega f_k^+ \quad (16)$$

where ω is the global electrophilicity index and f_k^- and f_k^+ are the nucleophilic and electrophilic Fukui functions. According to the Parr and Yang stated that sites in chemical compound or reactant with largest values of Fukui function (f_k) represent the high reactivity for corresponding attacks as compared to other atomic sites in the molecule or reactant. In the present study, the values of calculated Fukui functions (f_k) based on the Mulliken atomic charges and calculated at DFT/6-311++G(d,p) basis set in the gas phase, given in Table-5, indicates the most preferred reactive sites in the title molecule with reactivity order for the nucleophilic attacks (f_k^+) are S15 > S16 > C7 > C8 > C19 > C3> N14 > N13 >N30 > C9, for the electrophilic attacks are C1 > C35 > C17 > C4 and for free radical attacks are S16 > S15 > C24. The maximum values of local electrophilic descriptors (s_k^+ and ω_k^+) at S15 > S16 > C7>C3 and S15 > S16 > C7 > C8 indicate that these sites are more labile for nucleophilic attacks and maximum values of local nucleophilic descriptors (s_k^-, ω_k^-) at C1, C35 indicate that these sites are more labile for electrophilic attacks.

Atomic charge distribution (MPA): Mulliken atomic charge distribution on the molecule has an important role in the application of quantum chemical calculation to molecular system because this is influenced the electrophilic, nucleophilic

TABLE-5
FUKUI FUNCTION VALUES ON THE BASIS OF THE MULLIKEN ATOMIC CHARGES OF NEUTRAL, CATION AND ANION, THE FUKUI FUNCTIONS (f_k^+, f_k^-, f_k^0), LOCAL SOFTNESS (s_k^+, s_k^-) AND LOCAL PHILICITY (ω_k^+, ω_k^-) OF THE TITLE MOLECULE CALCULATED AT DFT/6-311++G(d,p) BASIS SET IN THE GAS PHASE

Atoms	q_k^0	q_k^+	q_k^-	f_k^+	f_k^-	f_k^0	s_k^+	s_k^-	ω_k^+	ω_k^-
1C	0.259135	-0.425508	-0.501286	-0.6846	0.7604	0.0378	-0.1875	0.2083	-4.33890	4.81914
2C	-0.09425	-0.162232	-0.136238	-0.0679	0.0419	-0.0129	-0.0186	0.0115	-0.43077	0.26604
3C	-0.09413	0.084277	0.030894	0.1784	-0.1250	0.0266	0.0488	-0.0342	1.13064	-0.79233
4C	0.259005	0.115140	0.079285	-0.1438	0.1797	0.0179	-0.0394	0.0492	-0.91174	1.13896
6C	0.085789	0.170962	0.020798	0.0851	0.0649	0.0750	0.0233	0.0178	0.53978	0.41187
7C	0.085670	0.279706	0.109632	0.1940	-0.0239	0.0850	0.0531	-0.0065	1.22969	-0.15185
8C	-0.14327	0.031681	-0.087891	0.1749	-0.0553	0.0597	0.0479	-0.0151	1.10879	-0.35080
9C	-0.14324	-0.024330	-0.157191	0.1189	0.0139	0.0664	0.0325	0.0038	0.75362	0.08838
13N	0.25703	0.399119	0.224811	0.1420	0.0322	0.0871	0.0389	0.0088	0.90047	0.20419
14N	0.25705	0.408512	0.247586	0.1514	0.0094	0.0804	0.0415	0.0025	0.95987	0.05998
15S	-0.60397	0.127918	-0.078654	0.7318	-0.5253	0.1032	0.2005	-0.1439	4.63832	-3.32918
16S	-0.60435	0.022732	-0.343102	0.6270	-0.2612	0.1829	0.1718	-0.0715	3.97416	-1.65570
17C	-0.45062	-0.792274	-0.697886	-0.3416	0.2472	-0.0471	-0.0936	0.0677	-2.16521	1.56703
18C	0.17244	0.213911	0.105959	0.0414	0.0664	-0.1678	0.0113	0.0182	0.26278	0.42135
19C	0.05043	0.202099	0.066126	0.1516	-0.0156	0.0099	0.0415	-0.0042	0.96114	-0.09942
22C	-0.45015	-0.829482	-0.549631	-0.3773	0.0994	-0.1399	-0.1033	0.0272	-2.39132	0.63045
23C	0.17234	0.208654	0.182234	0.0363	-0.0098	0.0132	0.0099	-0.0027	0.23012	-0.06269
24C	0.05057	0.135004	-0.046066	0.0844	0.0966	0.0905	0.0231	0.0264	0.53505	0.61246
27N	0.03844	0.081069	0.020828	0.0426	0.0176	0.0301	0.0116	0.0048	0.27010	0.11166
28N	0.27631	0.349619	0.337492	0.0733	-0.0611	0.0060	0.0200	-0.0167	0.46453	-0.38768
29N	0.27630	0.243498	0.218097	-0.0328	0.0582	0.0127	-0.0089	0.0159	-0.20792	0.36890
30N	0.03841	0.158545	0.121046	0.1201	-0.0826	0.0187	0.0329	-0.0226	0.76133	-0.52369
31C	0.15256	0.230183	0.176865	0.0776	-0.0243	0.0266	0.0212	-0.0066	0.49190	-0.15400
35C	0.15247	-0.228803	-0.343707	-0.3813	0.4961	0.0574	-0.1044	0.1359	-2.41690	3.14456

nature, nuclear magnetic resonance (NMR) chemical shifts, vibrational spectra, dipole moment, molecular polarizability, electronic structure, global and local chemical activities and a lot of properties of molecular systems. Mulliken population analyses also are an important factor in structure-property (SPR) and structure-activity relations (SARs). The atomic charge distribution over the atom recommends the formation of donor and acceptor pairs require the charge transfer in the molecule [61]. The atomic charges of the title molecule were calculated using the MPA (Mulliken population analysis) [62]. The Mulliken population analysis of the title molecule was calculated using DFT/6-311++G(d,p) basis set and are listed in Table-6 and results are plotted in Fig. 8. In general, atomic charges obtained by MPA are the basis set dependent and their absolute magnitude has little physical meaning [63]. In the present study, from Table-6 and Fig. 8, it is clear that the C1and N27 atom show negative charge in water solvent and positive charge in gas phase and C3 atom show opposite charges due to electronegative atoms and conjugations as well as hyperconjugation effect and only C4 atom show positive charge in the both phase. Rest of the carbon atoms (C2, C6, C7, C8, C9, C17, C18, C19, C22, C23, C24, C31 and C35) and the nitrogen atom except N27 show positive charges. The highest electronegative charge on carbon atoms and sulphur atoms order is C35 > C22 > C17 > S15 = S16 due to the delocalization of electronic charge, intermolecular hydrogen bonding increase the biological property.

Vibrational assignments: The title molecule (2,3-*bis*[(1-methyl-1*H*-imidazole-2-yl)sulfanyl]quinoxaline) contains 38 atoms, 184 electrons and have C1 point group symmetry with 108 normal mode of vibrations. All modes of vibration of the title molecule are studied with the help of the combination of VEDA 4.0 program package and Gauss View 5.0 program. The detailed vibrational assignment of the title molecule of theoretically calculated wavenumbers (cm^{-1}) is based on normal mode analyses and calculated by DFT/B3LYP/6-311++G(d,p) basis set. The IR spectrum of title molecule is shown in Fig. 9. The unscaled theoretical frequencies and wavenumbers using DFT method with potential energy distributions (PEDs) are listed in Table-7.

C-H vibrations: The heteroaromatic and aromatic compounds, the C-H stretching vibrations appear in the range of 3100-3000 cm^{-1} [32,64], in this region, the vibrations are not affected by the nature of the substituent's while C-H in-plane and out-of-plane bending vibrations were observed in the range 1300-1000 cm^{-1} and 900-675 cm^{-1} [65], respectively. In the present study, the C-H stretching band of quinoxaline ring of the title molecule is calculated at DFT level at 3336.65-3264.79 cm^{-1} with PED 14 %. The C-H stretching vibrations of imidazole rings of title molecule are calculated at DFT method at 3395.43-

TABLE-6
MULLIKEN ATOMIC CHARGES AT DIFFERENT ATOMIC SITES OF TITLE MOLECULE CALCULATED USING DFT/6-311++G(d,p) METHODS IN THE GAS PHASE AND WATER SOLVENT USING IEF-PCM MODEL

Atoms	Gas phase	Water	Atoms	Gas phase	Water	Atoms	Gas phase	Water
1C	0.259135	-0.323235	14N	0.257051	0.314395	27N	0.038448	-0.065294
2C	-0.094259	-0.132833	15S	-0.603971	-0.108053	28N	0.276319	0.329742
3C	-0.094130	0.117836	16S	-0.604358	-0.069852	29N	0.276307	0.194456
4C	0.259005	0.199327	17C	-0.450621	-0.687327	30N	0.038412	0.002180
5H	0.175337	0.231878	18C	-0.008221	-0.088563	31C	-0.366894	-0.312414
6C	-0.089548	-0.174205	19C	-0.106645	-0.060390	32H	0.212621	0.172341
7C	-0.089645	-0.033431	20H	0.180668	0.230483	33H	0.144829	0.196225
8C	-0.320699	-0.254304	21H	0.157083	0.207424	34H	0.162007	0.167816
9C	-0.320665	-0.284225	22C	-0.450151	-0.632421	35C	-0.366987	-1.000885
10H	0.173515	0.218501	23C	-0.008314	-0.074706	36H	0.212629	0.226592
11H	0.177421	0.223337	24C	-0.106521	-0.123250	37H	0.144837	0.185749
12H	0.177420	0.215906	25H	0.180656	0.225644	38H	0.162000	0.280242
13N	0.257031	0.263930	26H	0.157096	0.221385	–	–	–

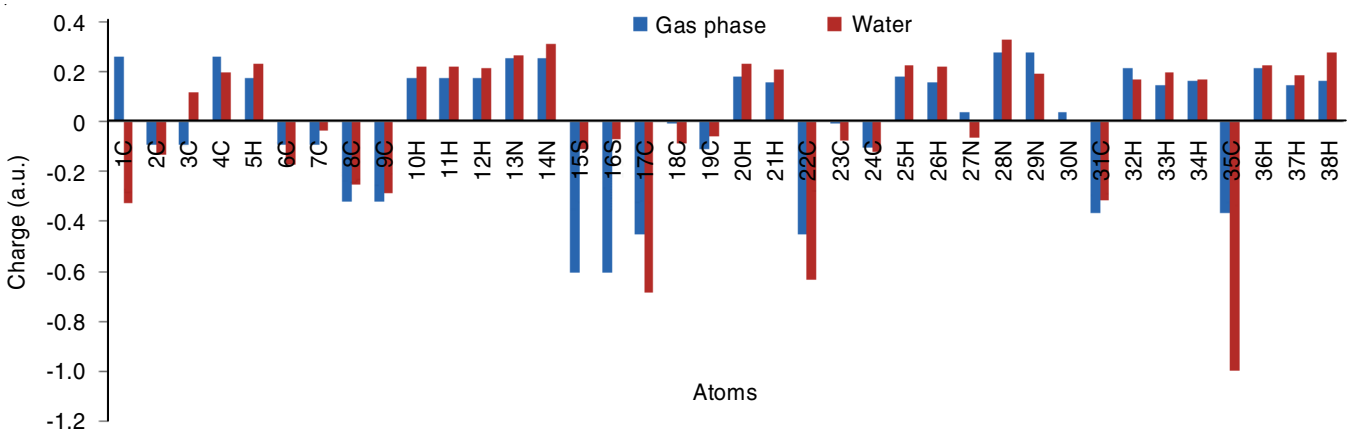

Fig. 8. Mulliken atomic charges distribution of the title molecule calculated using DFT/6-311++G(d,p) methods in the gas phase and water solvent phase

TABLE-7
CALCULATED VIBRATIONAL WAVENUMBERS (cm^{-1}) OF THE TITLE MOLECULE USING DFT/B3LYP/6-311++G(d,p) METHOD IN GAS PHASE

S. No.	Wave numbers (cm^{-1})	IR intensity	Vibrational assignments increasing order of PED (PED ≥ 10 %)	S. No.	Wave numbers (cm^{-1})	IR intensity	Vibrational assignments increasing order of PED (PED ≥ 10 %)
1	8.4527	2.6821	β_{out} (NCCN)P (15)	55	874.0246	0.6227	β(HCC)R1
2	14.7405	0.8150	β_{out} (CCNN)P (10)	56	875.2007	10.5729	β(HCN)P1 (16)
3	19.1446	1.0336	β_{out} (CCSN)P (13)	57	905.3072	3.8581	β(HCH)P2 (10)
4	27.6659	6.4466	β_{out} (CNSC) (21)	58	922.5352	63.0167	β(CCH)R2
5	35.1962	6.8226	β_{out} (CCNN) (14)	59	924.1965	11.9066	β(CNC)P1 (39)
6	40.7368	3.0395	β_{out} (CNCS) (19)	60	962.9431	0.3305	β(CCC)R1
7	51.2770	0.0802	β_{out} (CCNN) (47)	61	993.9718	100.7235	β(CSC) + ν_s (S15-C17) (14)
8	65.2885	0.5168	β_{out} (CCSN) (11)	62	1012.3135	34.2141	β(CNC) (14)
9	74.4768	1.3921	β_{out} (CCSN) (10)	63	1023.3578	76.7040	β(CSC) (12) + ν_s (C4-S16) (10)
10	81.9731	1.0668	ρ(CCSC) (33)	64	1034.8776	37.6160	β(NNC)R2
11	117.6714	3.0029	ρ(CCCN) (16)	65	1062.4632	18.2666	β(NCC)P2
12	146.1260	2.7315	β_{out}(CNCC) (10)	66	1064.3848	4.8298	β(CNC)P2 (10)
13	156.2236	0.2861	ρ(CNHC) (43)	67	1081.5259	23.4926	β(CCN)P1 (72)
14	175.1582	0.8251	ρ(CNHC)	68	1104.0185	3.0359	β(HCC)P2 (10)
15	197.5250	0.3900	β_{out}(CCNC) (10)	69	1136.5133	19.7245	β(HCC)P1 (68)
16	238.5616	1.2889	β_{out}(CCNC) (10)	70	1149.6365	37.4204	β(CNH)P2
17	266.8069	0.0277	ρ(HCHN) (10)	71	1167.5339	10.3203	β(HCN)P2 (11)
18	284.4327	14.7450	ρ(HCCN) (12)	72	1170.9010	0.3962	ν_{as} (C8-C9)R1 (29)
19	308.5117	1.3676	ρ(HCCN) (12)	73	1190.8916	29.8003	ν_{as} (N28-C35)P2 (11)
20	329.2219	5.0648	ρ(HCCC) (12) + β_{out} (CCC)	74	1227.1967	1.3650	ν_{as} (C2-C3)R1 (10)
21	361.0110	3.5221	ρ(HCCC) (13)	75	1243.3789	18.3134	ν_s (C2-C3)R1
22	371.2023	3.4227	ρ(HCCC) (26)	76	1260.4168	6.3011	ν_s (C23-C24)P2
23	380.5369	10.1036	ρ(HCCC) (29) + β_{out}(CCC)	77	1269.7226	25.2705	ν_{as} (C35-H)P2 (23)
24	412.0709	8.8315	ρ(HCCC) (17)	78	1274.0375	1.0155	ν_s (C18-C19)P1
25	432.1403	3.5011	ρ(HCNC) (13)	79	1348.7577	8.9940	ν_{as} (C8-C9)R1 (26)
26	455.9379	20.5013	β_{out}(CCNS) (10) + ν_s (S16-C22)	80	1356.5190	7.4986	ν_{as} (C8-C9)R1 (15), ν_s(C1-S15) (15)
27	476.1664	6.3050	ρ(HCHS) (14) + ν_{as} (S16-C22)	81	1368.5000	1.8246	ν_s (N28-C35)P1 (11)
28	489.5794	1.7036	ρ(HCHN) (13)	82	1407.2075	12.1240	ν_s (C31-N29)P2
29	530.3011	21.6635	ρ(HCHS) (20) + ν_{as} (S15-C17)	83	1435.4607	54.3450	ν_s (N27-C17)P1 (15)
30	558.7084	9.6756	ρ(NHCN) (49)	84	1440.8861	61.0258	ν_s (N30-C22)P2
31	576.9890	2.1698	ρ(CNSC) (36) + ν_s (C4-S16)	85	1447.3286	16.4389	ν_s (C1-N13)R2 (14)
32	586.0026	1.4287	ρ(HCHC) (15)	86	1462.0061	5.8848	ν_s (C35-H38)P1 (10)
33	591.5219	2.8415	ρ(HCCN) (68)	87	1470.6097	13.2998	ν_{as} (C31-H37)P2 (16)
34	600.8233	4.6264	ρ(HCNC) (16)	88	1478.1829	5.8572	ν_s (C31-H36)P2 (14)
35	611.2890	6.3221	ρ(CNHC) + ν_s	89	1527.0936	60.9698	ν_{as} (C1-N13)R2 (18)
36	663.9086	12.2830	β(CNH) (10)	90	1575.2679	0.4376	ν_{as} (C23-C24)P2 (14)
37	672.3497	32.6511	β (CCC)	91	1594.1706	21.2194	ν_s (C35-H)P1 (14)
38	676.9303	28.4659	β (CCN) (11)	92	1608.4996	19.4234	ν_s (C18-C19)P2 (14)
39	702.7215	6.5929	β (CNC) (14)	93	1621.1390	6.9546	ν_s (C3-C7)R1
40	717.9423	9.0647	β (CCC) (26)	94	1644.9960	3.5926	ν_s (C6-C8)R1 (13)
41	725.6490	22.9101	β (CCC) (21)	95	3148.9668	60.0073	ν_{as} (C8-^{1}H1)R1 (17)
42	732.9950	10.6345	β (CNC) (11)	96	3200.7817	32.4561	ν_s (C31-H)P2 (28)
43	737.2021	82.0512	β (NHC)	97	3211.7843	18.9965	ν_s(C35-H)P1
44	765.7221	17.0979	β_{out} (HCC) (10)	98	3262.6627	0.2762	ν_{as}(C19-H21)P1 (15)
45	771.3343	7.6143	β (HCC) (10)	99	3264.7909	5.9416	ν_s(C9-^{1}H2)R1 (12)
46	799.5866	3.2390	β (HCC) (18)	100	3273.4397	15.9462	ν_{as}(C31-H32)P2 (15)
47	805.9192	7.4101	β (HCC) (33)	101	3304.5692	19.7110	ν_s(C35-H37)P1
48	810.6123	6.9919	β (HCH)	102	3310.5076	0.5457	ν_{as} (C7-^{1}H0)R1
49	830.7896	15.8560	β (HCN) (10)	103	3310.7918	0.1465	ν_{as} (C24-H26)P2 (11)
50	838.3033	1.0959	β_{out} (HCH) (10)	104	3336.6569	1.0045	ν_s(C6-H5)R1 (14)
51	839.0077	2.4260	β (NCS) (36) + ν_s (C1-S15)	105	3353.1498	11.6527	ν_{as}C31-H33)P2
52	844.0240	0.4812	β (CCN) (31)	106	3366.0242	47.4593	ν_{as}(C35-H37)P1 (19)
53	852.2179	25.4697	β(HCN) (11)	107	3385.1612	1.9075	ν_s (C18-H20)P1
54	862.1778	0.8843	β(HCC)	108	3395.4320	2.9647	ν_s (C23-H25)P2 (23)

Abbreviations: ν, stretching; s, symmetric; as, asymmetric; β, in-plane bending; β_{out}, out-of-plane bending; ρ, torsion; R1, R2, quinoxaline ring; P1, P2, imidazole ring.

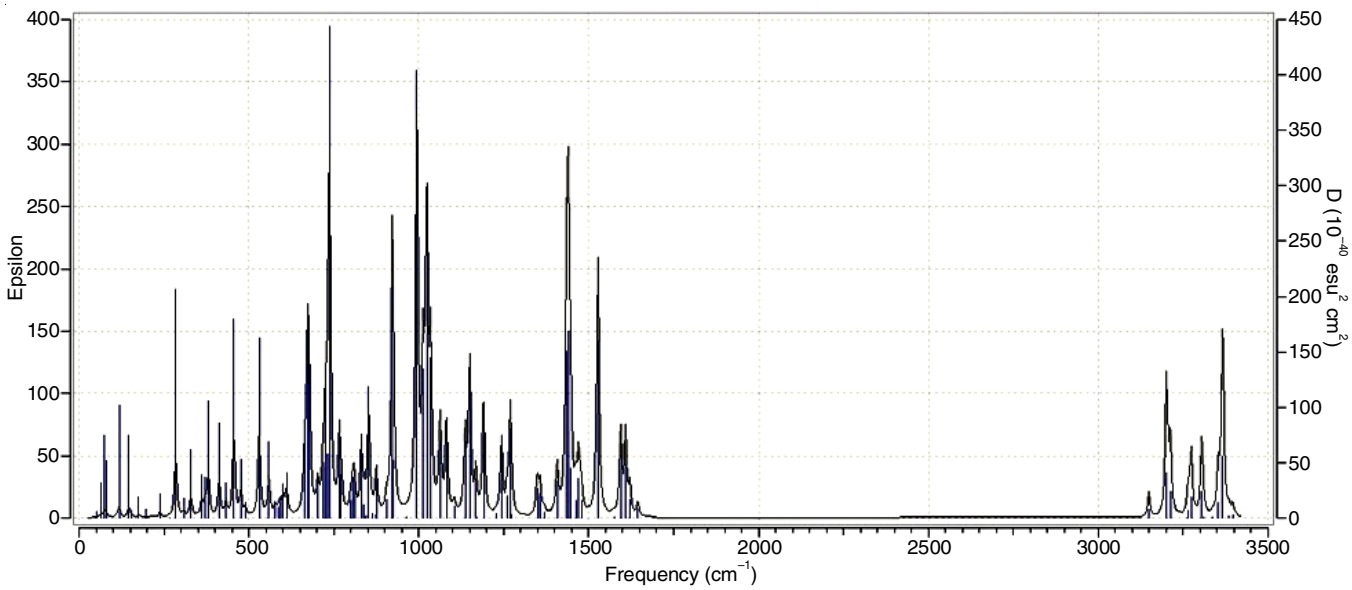

Fig. 9. Calculated IR spectrum of the title molecule at DFT/B3LYP/6-311++G(d,p) level of theory in the gas phase

3200.78 cm^{-1} with PED 28 %. The C-H in-plane bending vibration was calculated at DFT method in the range of 1136.51-862.17 cm^{-1} while the out-of-plane bending vibrations are appear at DFT level at 838.30-763.73 cm^{-1}.

C-C and C-N vibrations: The C-C stretching bands appeared in the region at 1625-1400 cm^{-1} [66]. Here the wavenumbers of title molecule were calculated at DFT level occurring in the region 1644.99-1260.41 cm^{-1}. The C-C-C deformation in-plane and out-of-plane bands occur in the region at 641-509 cm^{-1} and at 477-282 cm^{-1}, respectively [67]. Here the wavenumbers were calculated at DFT level in the region 725.64-672.34 cm^{-1} and 380.53-329.22 cm^{-1} for in-plane and out-of-plane bending deformation, respectively. The C-N bands identification is difficult task because of the mixing of several bands. Silverstein [68] assigned C-N stretching vibrations occurring in the region 1382-1266 cm^{-1} for aromatic amines. Karabacak *et al.* [69] assigned C=N and C-N stretching vibrations at 1689 and 1302 cm^{-1}, respectively in the FT-IR spectrum. In the present work, the bands are calculated at DFT level at the region 1447.32-1368.50 cm^{-1}.

C-S vibrations: The C-S band stretching bands identification is difficult and also unpredictable. Since the title molecule contains a quinoxaline ring substituted with sulfanyl group. The C-S stretching vibrations occur in the region 700-600 cm^{-1} [68]. The C-S stretching bands were calculated at DFT level at the region 1356.51-455.93 cm^{-1} has dominant contribution assigned by TED [69].

NMR spectroscopy and calculations: The accurate predictions of molecular geometries are essential for reliable calculation of magnetic properties, in the identification of ionic species. The theoretical ^{1}H and ^{13}C NMR spectra of title molecule in gas and solution phase (water, DMSO and $CHCl_3$) using IEF-PCM model were calculated by using DFT/6-311++G(d,p) basis set with GIAO method and spectra and chemical shifts are presented in Figs. 10 & 11 and Table-8. In the present study, the ^{1}H and ^{13}C chemical shifts of the title molecule were referenced by the corresponding values of TMS, which was calculated using B3LYP/6-311+G (2d,p) with GIAO level of theory.

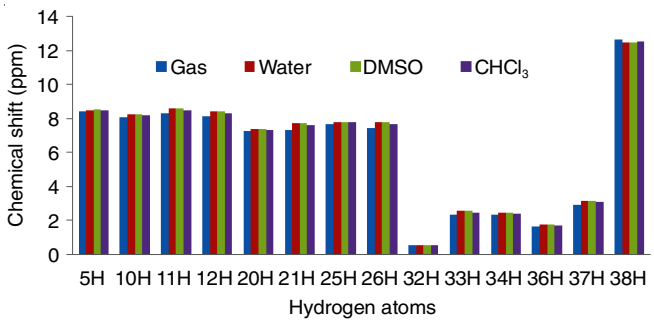

Fig. 10. Calculated ^{13}C NMR spectrum of the title molecule using DFT/6-311++G(d,p) level of theory in the gas phase and solvent phase (water, DMSO and $CHCl_3$)

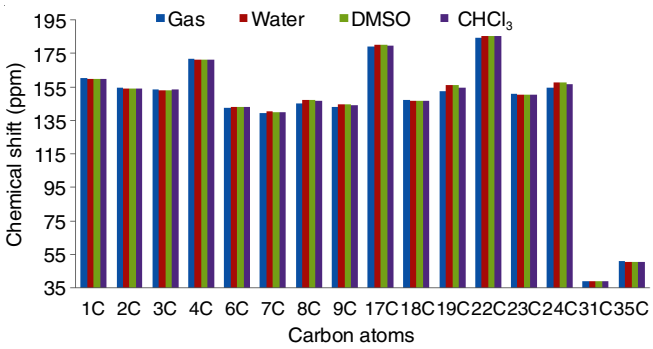

Fig. 11. Calculated ^{13}C NMR spectrum of the title molecule using DFT/6-311++G(d,p) level of theory in the gas phase and solvent phase (water, DMSO and $CHCl_3$)

In the present investigation, the ^{13}C chemical shifts of title molecule in the gas phase, water, DMSO and chloroform of C22 (=184.34, 185.51, 185.49 and 185.14 ppm), C17 (=178.98, 180.05, 180.03 and 179.76 ppm) and C4 (=171.57, 171.10, 171.11 and 171.19 ppm), C1 (=160.39, 159.57, 159.57 and 159.52 ppm), respectively, are greater than other carbon atoms because of deshielded N and S atoms in quinoxaline ring and imidazole rings. Similarly, 1H isotropic chemical shifts proton numbered H38 (12.69 ppm in the gas phase), 1H1 (=8.61 ppm in water), H5, 1H0 and 1H2 values are higher than the other

TABLE-8
THEORETICAL PROBABLE ^{13}C AND ^{1}H NMR CHEMICAL SHIFTS [WITH RESPECT TO TMS AND IN GAS PHASE AND SOLVENT (WATER, DMSO, $CHCl_3$)] OF TITLE MOLECULE USING DFT/6-311++G(d,p) BASIS SET

^{13}C NMR					^{1}H NMR				
Nucleus	Gas (ppm)	Water (ppm)	DMSO (ppm)	$CHCl_3$ (ppm)	Nucleus	Gas (ppm)	Water (ppm)	DMSO (ppm)	$CHCl_3$ (ppm)
1C	160.39	159.57	159.57	159.52	5H	8.40	8.51	8.52	8.51
2C	154.37	153.77	153.78	153.92	10H	8.09	8.23	8.24	8.20
3C	153.73	153.13	153.14	153.28	11H	8.29	8.61	8.60	8.51
4C	171.57	171.10	171.11	171.19	12H	8.12	8.42	8.41	8.33
6C	142.53	143.26	143.26	143.14	20H	7.29	7.36	7.37	7.34
7C	139.36	140.17	140.16	139.97	21H	7.35	7.75	7.76	7.62
8C	145.08	147.20	147.17	146.53	25H	7.69	7.80	7.80	7.77
9C	142.82	144.75	144.72	144.15	26H	7.44	7.80	7.80	7.68
17C	178.98	180.05	180.03	179.76	32H	0.56	0.53	0.53	0.55
18C	147.21	146.46	146.47	146.72	33H	2.33	2.55	2.55	2.47
19C	152.43	155.99	155.92	154.75	34H	2.33	2.45	2.45	2.40
22C	184.34	185.51	185.49	185.14	36H	1.64	1.75	1.74	1.71
23C	150.73	150.15	150.16	150.35	37H	2.91	3.16	3.16	3.08
24C	154.43	157.46	157.41	156.42	38H	12.69	12.47	12.48	12.55
31C	38.85	39.12	39.13	39.01	–	–	–	–	–
35C	50.85	50.66	50.67	50.69	–	–	–	–	–

hydrogen atoms in the title molecule due to electronic charge density around these atoms were higher than the others. In this study, the solvent effects on the title molecule of ^{1}H and ^{13}C chemical shifts exhibited more multiplets because the title molecule was affected by solvent (water, DMSO and chloroform).

Non-linear optical properties (NLO) and dipole moment: Non-linear optical active materials have more importance in the present scenario of research due to providing key functions of optical switching, laser, fiber, optical modulation, frequency shifting, optical material logic, strength of molecular interactions, collision processes and optical memory for appearing technologies in the area of telecommunications, optical interconnections and signal processing [70,71]. It is well known that the higher value of polarizability (α), hyperpolarizability (β) and dipole moment (μ_{tot}) are important for more active NLO material. In the present study, the electronic dipole moment (μ_{tot}), molecular polarizability (α_{tot}), anisotropy of polarizability ($\Delta\alpha$) and molecular first hyperpolarizability (β_{tot}) of the title molecule were investigated and calculated by finite field approach using DFT/B3LYP/6-311++G(d,p) basis set in gas phase available in Gaussian 09 Revision-A.02 program package. The frequency job output file of Gaussian was used for the calculation of polarizability and hyperpolarizability tensor (α_{xx}, α_{yy}, α_{zz}, α_{xy}, α_{yz}, α_{zx} and β_{xxx}, β_{xxy}, β_{xxz}, β_{yyy}, β_{yyz}, β_{yyx}, β_{xyz}, β_{xzz}, β_{zzz}, β_{yzz}). The polarizability and hyperpolarizability values of the Gaussian output results are in atomic units (α; 1 a.u. = 0.1482 $\times 10^{-24}$ esu, β; 1 a.u. = 8.6393 $\times 10^{-33}$ esu) so they have been converted into the electronic units (esu). The mathematical equations of total static dipole moment (μ_{tot}), the total mean polarizability (α_{tot}), the anisotropy of polarizability ($\Delta\alpha$) and the mean first hyperpolarizability (β_{tot}) can be calculated using equations expressed as [32]:

$$\mu_{tot} = \Delta\mu^2_x + \mu^2_y + \mu^2_z \quad (17)$$

where μ_x, μ_y, μ_z are x, y, z components of dipole moment.

$$\alpha_{tot} = 1/3[\alpha_{xx} + \alpha_{yy} + \alpha_{zz}] \quad (18)$$

where α_{xx}, α_{yy}, α_{zz} are the components of the polarizability in xx, yy, zz planes.

$$\Delta\alpha = 1/\sqrt{2}\,[(\alpha_{xx} - \alpha_{yy})^2 + (\alpha_{yy} - \alpha_{zz})^2 + (\alpha_{zz} - \alpha_{xx})^2 + 6\alpha^2_{xz} + 6\alpha^2_{xy} + 6\alpha^2_{yz}]^{1/2} \quad (19)$$

$$\beta_{tot} = (\beta^2_x + \beta^2_y + \beta^2_z)^{1/2} \quad (20)$$

$$\beta_{tot} = [(\beta_{xxx} + \beta_{xyy} + \beta_{xzz})^2 + (\beta_{yyy} + \beta_{yxx} + \beta_{yzz})^2 + (\beta_{zzz} + \beta_{zxx} + \beta_{zyy})^2]^{1/2} \quad (21)$$

All the above electronic moments are presented in Table-9. The dipole moment, mean polarizability (α_{tot}) and anisotropy of polarizability ($\Delta\alpha$) of the title molecule are found to be 4.7259 D, 44.0298742 $\times 10^{-24}$ esu and 20.4778204 $\times 10^{-24}$ esu, respectively. The lowest value of dipole moment found for μ_x components, in this direction, this value equals to -4.0793 D. The calculated first static hyperpolarizability (β_{tot}) value equals to 1503.06255 $\times 10^{-33}$ esu because the magnitude of β_{tot} is one of

TABLE-9
CALCULATED VALUE OF DIPOLE MOMENT (μ_{tot}), MEAN POLARIZABILITY (α_{tot}), ANISOTROPY OF THE POLARIZABILITY ($\Delta\alpha$) COMPONENTS AND FIRST STATIC HYPERPOLARIZABILITY (β_{tot}) VALUE OF TITLE COMPOUND AT DFT/B3LYP/6-311++G(d,p) IN GAS PHASE

Dipole moment (μ_{tot})		First static hyperpolarizability	
μ_x	-4.0793	β_{xxx}	-122.3462
μ_y	1.7091	β_{xxy}	-54.7204
μ_z	-1.6649	β_{xyy}	-30.1704
μ_{tot}	4.7259	β_{yyy}	113.1136
Polarizability (α_{tot})		β_{xxz}	-46.2424
α_{xx}	330.989	β_{xyz}	31.5933
α_{xy}	-4.668	β_{yyz}	-27.7515
α_{yy}	354.333	β_{xzz}	0.7536
α_{xz}	11.285	β_{yzz}	-13.6412
α_{yz}	2.270	β_{zzz}	1.6463
α_{zz}	205.971	β_{tot} (a.u.)	173.979668
α_{tot} (esu)	44.0298742 $\times 10^{-24}$	β_{tot} (esu)	1503.06255 $\times 10^{-33}$
$\Delta\alpha$ (esu)	20.4778204 $\times 10^{-24}$	–	–

the key factors in NLO system. All the electronic moments of title molecule like dipole moment, polarizability and hyperpolarizability 3 times, 39 times and 717 times greater than the urea molecule because urea is the prototypical molecule used frequently as the threshold value for comparative purpose. The μ, α and β values of urea is 1.525686 Debye, 5.0477×10^{-24} esu and 780.324×10^{-33} esu. In the theoretical calculations, the β components are very useful as clarify the direction of charge delocalization. The largest β_{yyy} value of the title molecule indicates charge delocalization is along the bond axis. These results indicate that the title molecule is good candidate for NLO material.

Thermodynamic properties: The partition function is the most important parameters of thermodynamics. The partition function helps the study of thermodynamics, quantum theory and spectroscopy. The different types of partition function are (i) vibrational partition function (ii) electronic partition function (iii) translational partition function and (iv) rotational partition function.

The partition function is helpful in the study of enthalpy, total heat capacity, entropies, equilibrium constant and rate constant. The total energy of molecule is the sum of vibrational, electronic, translational, rotational partition function *i.e.* $E = E_v + E_e + E_t + E_r$. The statistical thermodynamical study of the title molecule have been calculated at room temperature 298.15 K and 1 atm pressure using DFT/B3LYP/6-311++G(d,p) basis set in the gas phase and results listed in Table-10. The total energy and total entropy were calculated at DFT to be about -1743.0714 a.u. and 133.692 cal/mol Kelvin, respectively. Moreover, it was found that the title molecule has highest heat capacity, zero-point vibrational energy and thermal energy at DFT level is 72.974 cal/mol Kelvin, 172.14851 Kcal/mol and 183.079 Kcal/mol, respectively. Herein, all the thermodynamical data gives helpful information about thermodynamic energies and estimate the direction of chemical reactions according to the second law of thermodynamics in the thermo-chemistry [72]. In this work, the thermodynamical studies have been performed only in the gas phase.

***in silico* Bioactivity evaluation & pharmacological investigation results:** The bioactivity score of the title molecule and ciprofloxacin in term of biological properties like GPCR ligand, ion channel modulator, kinase inhibitor, nuclear receptor ligand, protease inhibitor and enzyme inhibitor are predicted by calculating the activity score by molinspiration and are listed in Table-11 and biological activity are measured by activity score categorized under three different ranges: (i) if bioactivity score more than 0.00, having considerable biological activity, (ii) if bioactivity score 0.5 to 0.00, having moderately biological activity and (iii) if bioactivity is less than -0.50, having inactivity [73]. The results of this study found that the title molecule is biologically active and have physiological effects and compared with reference drug ciprofloxacin and comparative results are shown in Fig. 12.

TABLE-10
THERMODYNAMIC PROPERTIES OF THE TITLE MOLECULE CALCULATED AT TEMPERATURE 298.15 K AND 1 atm PRESSURE USING DFT/6-311++G(d,p) BASIS SET IN THE GAS PHASE

Properties		DFT
Total energy (a.u.)		-1743.0714
Rotational constant (GHz):	x	0.21804
	y	0.18509
	z	0.11409
E (enthalpy) (Kcal mol^{-1})		183.079
Heat capacity (Cv) (cal. mol^{-1} $Kelvin^{-1}$)		72.974
Entropy (S) (cal. mol^{-1} $Kelvin^{-1}$)		133.692
ZPVE (Kcal mol^{-1})		172.14851

Note: ZPVE = Zero point vibrational energy.

TABLE-11
BIOACTIVITY SCORE PREDICTION OF THE TITLE MOLECULE AND CIPROFLOXACIN FROM MOLINSPIRATION ONLINE SERVER

Bioactivity	Title molecule	Ciprofloxacin
GPCR ligand	-0.14	0.12
Ion channel modulator	-0.32	-0.04
Kinase inhibitor	0.09	-0.07
Nuclear receptor ligand	-0.47	-0.19
Protease inhibitor	-0.25	-0.20
Enzyme inhibitor	0.10	0.28

The drug-likeness and physico-chemical properties of the title molecule and reference drug ciprofloxacin are listed in Table-12 and the physico-chemical and drug likeness properties were calculated from Molinspiration server, ACD/ChemSketch, preADME server and molsoft server. The title molecule was

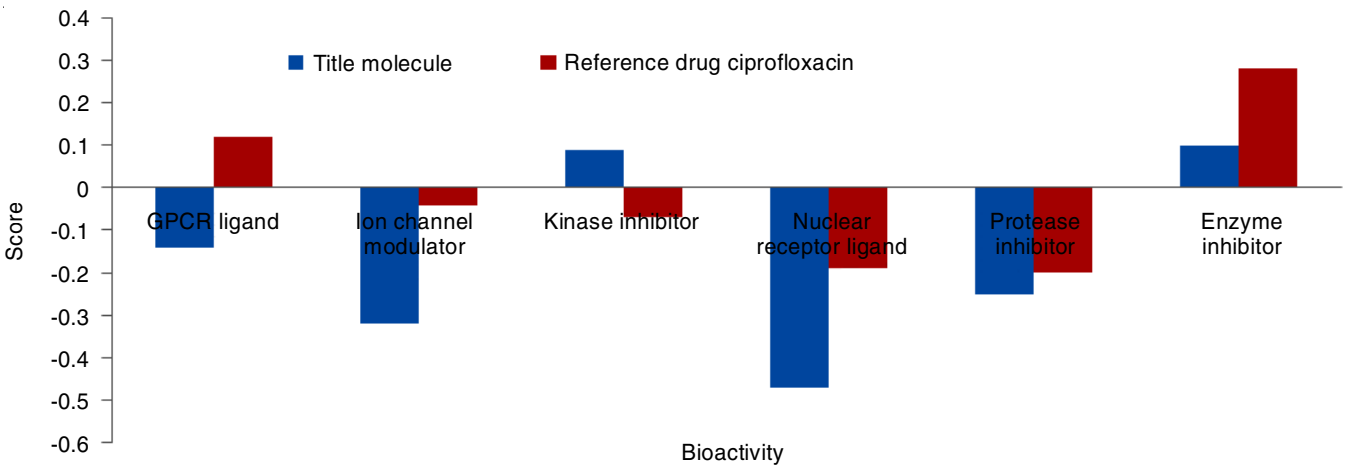

Fig. 12. Bioactivity chart of the title molecule and reference drug ciprofloxacin

TABLE-12
in silico PHYSICO-CHEMICAL PHARMACOKINETIC PARAMETERS IMPORTANT FOR GOOD ORAL BIOAVAILABILITY OF THE TITLE MOLECULE AND COMPARED WITH REFERENCE DRUG CIPROFLOXACIN

Physico-chemical properties					
Ligands	[a]MiLog $P_{o/w}$	[b]MW	CTPSA	[d]M. Volume	[e]mLog S
Title molecule	3.33	354.45	61.44	294.34	-2.86
Ciprofloxacin	-0.70	331.35	74.57	285.46	-2.96
Ligands	[f]MR (cm^3)	[g]d (gm/cm^3)	Hα (cm^3)	[i]γ (dyne/cm)	[j]Pr (cm^3)
Title molecule	94.76	1.45	40.22	62.0	684.1
Ciprofloxacin	95.25	1.46	33.00	67.4	649.7
Ligands	[k]nRB	[l]nHBD	[m]nHBA	[n]n	
Title molecule	4	0	6	1.771	
Ciprofloxacin	3	2	6	1.655	
Drug likeness properties					
Ligands	Lipinski rule of five violations	CMC like rule violations	Lead like rule violations	MDDR like rule violations	WDI like rule violations
Title molecule	0	0	0	0	0
Ciprofloxacin	0	0	0	0	0
Ligands	Bioavailability score	Drug likeness score	[o]%ABS	[p]SA	
Title molecule	0.55	-0.60	87.8032	3.01	
Ciprofloxacin	0.55	0.93	83.2734	2.51	

Description and acceptable range: [a]Predicted Moleinspiration octanol-water partition coefficient (log $P_{o/w}$) (≤ 5); [b]Molecular weight (≤ 500); CTopological polar surface area (TPSA) (160 Å); [d]Molar volume; [e]Logarithm of aqueous solubility (log S) (-6 to 0.5); [f]Molar refractivity (40-130 cm^3); [g]Density (d); HPolarizability (α); [i]Surface tension ((γ); [j]Parachor (Pr); [k]no. of Rotable bond (nRB); [l]no. of hydrogen bond donor (nHBD) (≤ 5); [m]no. of hydrogen bond acceptor (nHBA) (≤ 10); [n]Index of refraction (n); [o]Percentage human oral absorption (%ABS) (>80 % is high, <25 % is poor); [p]Synthetic accessibility (SA) 1 (very easy) to 10 (very difficult).

found in compliance with Lipinski's rule of five [74], CMC like rule, MDDR like rule and WDI (world drug index) like rule and lead like rule recommendations for novel chemical entity to have good oral bioavailability with no violations shows good agreement with ciprofloxacin. The miLog P value of title molecule and ciprofloxacin were found lower than the five, denote that the molecule will have good permeability across the cell membrane which in turn is required for production of bioactivity. For the title molecule the TPSA (topological polar surface area) value below 160 Å, which confirm that the title molecule is satisfying the optical requirement for drug absorption and showing good agreement with the reference drug. The Lipinski's "rule of five" states that a candidate molecule will likely to be active if (1) MW ≤ 500, (2) log P ≤ 5, (3) number of HBD ≤ 5 and (4) number of HBA ≤ 10. The title molecule and ciprofloxacin did not violet the any Lipinski rule of five and CMC like rule, WDI like rule, lead like rule and MDDR like rule calculated from preADME server and shows good physicochemical activity and drug likeness score. The topological polar surface area (TPSA) used to calculate the %ABS (percentage absorption) is equal to [109-(0.345 × TPSA) [75]. The title molecule and ciprofloxacin exhibited high %ABS is 87.8032 % and 83.2734 %, respectively. The molecular weight of title molecule and reference drug was less than 500 Daltons. The title molecule and reference drug possessed high number of rotatable bonds and therefore, exhibited conformational flexibility. The various physicochemical properties such as molar refractivity (MR), density (d), surface tension (γ), polarizability, parachor (Pr) and index of refraction (n) were evaluated by computational approach (ACD/ChemSketch (freeware) program. The molar refractivity (MR) value of the title molecule and ciprofloxacin is 94.76 and 95.25 cm^3 (acceptable range 40-130 cm^3) [76,77], respectively and other parameters exhibit good bioactivity score. The water solubility (m log S, log mol/L) score of the title molecule and drug is -2.86 and -2.96 mol/L calculated from the molsoft server. The synthetic accessibility score [acceptable range; from 1 (very easy) to 10 (very difficult)] of the title molecule and reference drug is 3.01 and 2.51, respectively. The bioavailability score and drug-likeness score of the title molecule and ciprofloxacin were calculated from siwssadme server and the molsoft server showed same score 0.55 and -0.60 and 0.93, respectively (Fig. 13).

The ADMET (absorption, distribution, metabolism, excretion and toxicity) properties of title molecule and ciprofloxacin were predicted by computational method listed in Tables 13 and 14. The ADMET, the absorption properties such as gastrointestinal absorption (GI), skin permeability (log Kp = cm/s) (Table-13), water solubility (log mol/L) and intestinal solubility (% abs) (Table-12) values justified that the selected title molecule have strong therapeutic potential and exhibit good agreement with reference drug ciprofloxacin. The results showed that the title molecule and drug more active and good GI absorption, water and intestinal solubility and skin permeability values (high and high), (-2.86 and -2.96 log mol/L) and (87.8032 and 83.2734 % abs) and (-6.43 and -9.09 cm/s), respectively. The literature study revealed that the molecule with percentage absorbance values less than 30 % considered as poorly absorbed molecule [78]. The title molecule and reference drug values showing much better results than slandered values 30 % abs and skin permeability slandered value -2.5 cm/s. The title molecule and reference drug ciprofloxacin are not BBB (blood brain barrier) permeant (Fig. 14), the yellow colour of boiled egg yolk both of the molecule predicted to passively permeate the blood-brain barrier (BBB). Human intestinal absorption (HIA) values of the title molecule and ciprofloxacin were 99.7206 and 96.2706 %, respectively indicating the highest percentage of absorption in the human intestine, while boiled egg showed

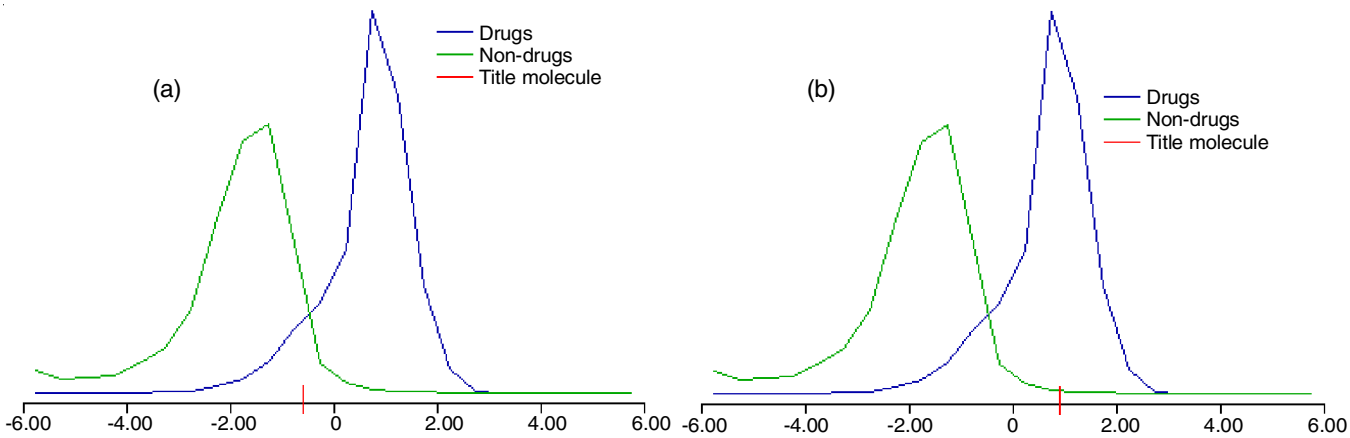

Fig. 13. (a) Drug likeness score chart of the title molecule and (b) reference drug ciprofloxacin, obtained from Molsoft server

TABLE-13
ABSORPTION, DISTRIBUTION, METABOLISM AND EXCRETION (ADME) PROPERTIES OF THE TITLE MOLECULE AND CIPROFLOXACIN

Properties	Title molecule	Ciprofloxacin
GI absorption	High	High
BBB permeant	No	No
BBB value	0.86719	0.01363
Buffer solubility (Mg/L)	22.325	32.7304
Caco2 (nm/s)	40.473	21.280
P-GP substrate	No	Yes
CYP1A2 inhibitor	Yes	No
CYP2C19 inhibitor	No	No
CYP 2C9 inhibitor	Yes	No
CYP2D6 inhibitor	Yes	No
CYP3A4 inhibitor	Yes	No
Log K_p (SP) (cm/s)	-6.43	-9.09
HIA (%)	99.7206	96.2706
MDCK (nm/s)	46.5133	10.3025
P. P. Binding (%)	97.304314	31.053958
PWS (Mg/L)	45.4497	251.438

TABLE-14
TOXICITY PROFILE OF THE TITLE COMPOUND AND CIPROFLOXACIN

Properties	Title compound	Ciprofloxacin
Acute algae toxicity	0.047523	0.07575
Ames test	Mutagen	Mutagen
Carcinogenicity (mouse)	N	N
Carcinogenicity (Rat)	N	N
Acute daphina toxicity	0.01615	0.2989
in vitro hERG inhibition	L-Risk	L-Risk
LD_{50} (mg/kg)/toxicity class	1000/4	2000/4
in vitro Ames test TA100 (+S9) strain (rat liver)	N	N
in vitro Ames test TA100 (-S9) strain	N	N
in vitro Ames test TA1535 (+S9) strain (rat liver)	N	P
in vitro Ames test TA1535 (-S9) strain	N	N
Hepatotoxicity	Inactive	Inactive

Note- P= Positive in test, N= Negative in test, M= Medium Risk, hERG= Human Ether-a-go-go-Related Gene (KCNH2 gene), Toxicity class-4 = harmful if swallowed ($300 < LD_{50} \leq 2000$ mg/kg)

both molecules passively absorbed by the gastrointestinal tract (Fig. 14) [79]. The blue dot showed by ciprofloxacin (Fig. 14) predicted to be effluated from the central nervous system by

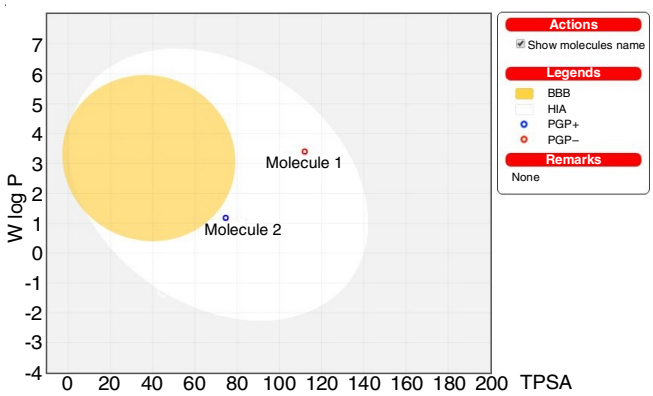

Fig. 14. Test and illustrative use of boiled egg: the title molecule (molecule-1) represented by red circle (well absorbed in human intestine and across the blood brain barrier) and molecule-2 (ref. drug ciprofloxacin) represented by blue color (well absorbed in the human intestine and positively bind with P-GPs)

the P-glycoprotein and red dot represent the title molecule predicted not to be effluated from the CNS by the P-glycoprotein's. The caco-2 cell permeability and MDCK cell permeability of title molecule and drug ciprofloxacin calculated at 7.4 pH the values are 40.473 and 21.280 nm/s and 46.5153 and 10.3025 nm/s, respectively. The results of caco-2 and MDCK cell permeability values showing middle permeable both of the molecules compared with standard value (value between 4 to 70 nm/s= middle permeable, value more than 70 nm/s = highest permeable). The title molecule shows 97.304314 % PPB (plasma protein binding) value which indicates the strong binding with plasma protein, whereas the drug ciprofloxacin, the PPB value is 31.053958 % which confirms very weak binding with plasma protein. On the other hand, the metabolic performance of the title molecule interaction with cytochrome P450 (CYP) protein [80] indicated that the title molecule were inhibitors of CYP1A2. CYP2C9, CYP2D6 and CYP3A4; this reduces the ability of these proteins to metabolize other drugs in the body of human and the title molecule is not inhibitor of CYP2C19 protein. The reference drug ciprofloxacin was not inhibitor of CYP P450 protein family. The title molecule not inhibited the P-glycoprotein's and this protein inhibited by the reference drug ciprofloxacin, a protein responsible for the absorption, distribution, metabolism and excretion of several drugs [81]. In relation to solubility in water and pure water, the title mole-

cule and ciprofloxacin achieved lower values of 45.4497 and 251.438 mg/L, respectively.

The toxicity profile of the title molecule and correlate with ciprofloxacin were calculated using preADMET server listed in Table-14. The identification of mutagenicity by Ames test indicated the mutagenicity data for both tested title molecule and reference drug. It is clear from the results that the title molecule shows antibacterial property like ciprofloxacin. However, in specific testing of title molecule and ciprofloxacin using TA100 and TA1535 (+S9 and –S9 strain of rat) cells, the results among the title molecule and ciprofloxacin were negative [82] and the title molecule and ciprofloxacin did not produce carcinogenicity in mice or rats. The computed LD_{50} dose in rat model revealed that the title molecule had almost the same LD_{50} toxicity class-4, compared with ciprofloxacin [83,84]. The computed hepatotoxicity of the title molecule and ciprofloxacin was shown non-toxicity. Likewise, the computed result of hERG channel inhibition for title molecule shows satisfactory results as compared with reference drug ciprofloxacin and both molecule shows low risk for hERG channel inhibition.

Molecular docking studies: Molecular docking is the most useful and reliable approach to explore the possible binding between protein and ligand complex. Imidazole containing quinoxaline derivatives were reported to inhibit biotin carboxylase of *E. coli* strain K-12 [85] and antibiotic resistant enzyme aminoglycoside phosphotransferase APH(2")IVA of *Enterococcus casseliflavus* [86]. Based on computational studies and compare with reference drug ciprofloxacin (antibacterial), the title molecule shows same physico-chemical and ADMET properties as ciprofloxacin. The antibacterial activity exhibited by the title molecule as reference drug ciprofloxacin, molecular docking studies were performed in the active site of biotin carboxylase of *E. coli* strain K12 and antibiotic resistant enzyme aminoglycoside phosphotranferase APH(2")IVA of *Enterococcus casseliflavus* to understand its mechanism of action with the title molecule and ciprofloxacin reference drug and results of docking listed in Table-15. *in silico* approaches like molecular docking have become very beneficial to identify the potential targets and active site for different ligands and are associated with thermodynamic interactions (hydrophobic interactions, van der Waal interaction, ionic interaction, hydrogen bonding and covalent interactions) with the target enzyme governing the inhibition of the target microorganism. The interactions of enzyme biotin carboxylase with the title molecule shows total energy and ligand-protein binding energy in term of moldock score and the rerank score is found to be 721.534, 4142.301, 684.701 and 4094.641 kcal/mol while the ciprofloxacin's score is 826.116, 4004.311, 794.341 and 3984.298 kcal/mol, respectively. The highest dock score indicates a good binding affinity of the ligand towards the target and *vice-versa*. It is also noted that the "protein-ligand" complex of title molecule and biotin carboxylase is stabilized by hydrogen binding and steric interactions (π-π interaction) involving amino acid like Lys116 (B), Lys159 (B), Gly164 (B), HOH2041 (81), 2044 (87) (B) and HOH2054 (B) (107), Asn (290), Gln (294), Glu (201, 211, 276, 288), Gly (163, 165, 166), His (209, 236), Ile (287), Leu (278), Lys (238), Met (169, 289), Phe (275, 277, 286), Thr 9274), Tyr (199, 285), Val (131), respectively and same as ciprofloxacin-biotin carboxylase complex hydrogen binding interactions and steric interactions (π-π interaction) are Asn290(B), Glu276, 288(B), Lys116(B), Thr274(B) and Ala272(B), Gln213, 294(B), Glu87, 211(B), Gly273(B), Ile212, 287, 293(B), Met113,289(B), Phe275, 286(B), Thr291 (B), Tyr269(B), Val214(B), HOH2041(B)81, respectively. The binding energy of title molecule and ciprofloxacin with aminoglycoside phosphotransferase APH(2")IVA shows total energy and ligand-protein complex energy in term of moldock score and rerank score are 186.387, 806.456, 177.027, 787.151, 570.108, 2286.137, 537.761 and 2265.559 kcal/mol, respectively. The hydrogen bonding and steric interactions for title molecule and ciprofloxacin with aminoglycoside phosphotransferase APH(2")IVA antibiotic resistant enzyme are Ser199(B), HOH580(B), Asn32, 196 (B) and Asp197, 201, 217, 220 (B),

TABLE-15
DOCKING PARAMETERS OF THE TITLE MOLECULE AND REFERENCE DRUG CIPROFLOXACIN DOCKED INTO THE ACTIVE SITES OF THE TARGET PROTEINS

Ligand ID	PDB ID	Total energy (Kcal/mol)		Protein-ligand interactions energy (Kcal/mol)		Binding sites/Targets
		Moldock score	Rerank score	Moldock score	Rerank score	Hydrogen bonds with water & amino acid residues/ID
Title molecule	2V59	721.534	4142.301	684.704	4094.144	HOH2054 (B) (107), Asn (290), Gln (294), Glu (201, 211, 276, 288), Gly (163, 164, 165, 166), His (209, 236), Ile (287), Leu (278), Lys (116, 159, 238), Met (169, 289), Phe (275, 277, 286), Thr 9274), Tyr (199, 285), Val (131), HOH2041 (B) (81), HOH2044 (B) (87)
	4DFU	186.387	806.456	177.027	787.151	H-Bonding: Ser199(B), HOH580(B), Asn32, 196 (B) Steric interaction: Asp197, 201, 217, 220 (B), His202 (B), Phe(198) (B), Ser232 (B), Lys267 (B), Trp271, 287 (B), Tyr278 (B), HOH523, 535, 556, 557, 560, 565, 571, 572 (B)
Ciprofloxacin	2V59	826.116	4004.311	794.341	3984.298	H-Bonding: Asn290(B), Glu276, 288(B), Lys116(B), Thr274(B) Steric interaction: Ala272(B), Gln213, 294(B), Glu87, 211(B), Gly273(B), Ile212, 287, 293(B), Met113,289(B), Phe275, 286(B), Thr291(B), Tyr269(B), Val214(B), HOH2041(B)81
	4DFU	570.108	2286.137	537.761	2265.559	H-Bonding: Asp197(B), Ser232(B), Phe198(B), Asp225(B), Pro226(B), Asn228(B), HOH535, 556, 557, 560, 571, 580(B) Steric interaction: Asn196(B), Asp220, 227, 229(B), His195, 202(B), Ile194, 231(B), Phe230(B), Pro230(B), Ser224(B), Lys267(B), HOH517, 544, 547, 565, 572, 581(B)

His202 (B), Phe(198) (B), Ser232 (B), Lys267 (B), Trp271, 287 (B), Tyr278 (B), HOH523, 535, 556, 557, 560, 565, 571, 572 (B) and Asp197(B), Ser232 (B), Phe198(B), Asp225(B), Pro226(B), Asn228(B), HOH535, 556, 557, 560, 571, 580(B) and Asn196(B), Asp220, 227, 229(B), His195, 202(B), Ile194, 231(B), Phe230(B), Pro230 (B), Ser224(B), Lys267(B), HOH517, 544, 547, 565, 572, 581 (B), respectively. All the results of tile molecule was to be close to that of ciprofloxacin, which as strongly suggests that the title molecule could serve as a pertinent starting point for the rational design of drugs targeting biotin carboxylase of *E. coli* strain K12 and aminoglycoside phosphotransferase APH(2")IVA antibiotic resistant protein of *Enterococcus casseliflavus*. The above finding suggests that the rationally designed newly title molecule might also act by the same mechanism. The docking pose, hydrogen bonding interactions and steric interactions of the title molecule and reference drug ciprofloxacin with biotin carboxylase and aminoglycoside phosphotransferase APH(2")IVA enzyme are shown in Fig. 15.

From Table-16, the best 4-ranked structures binding free energy (ΔG) of the title molecule and ciprofloxacin with biotin carboxylase protein and antibiotic resistant enzyme aminoglycoside phosphorylase APH(2")IVA of were estimated by ParDock server. The molecular docking studies revels that the title molecule binds at catalytic pocket of biotin carboxylase enzyme with binding energy of -4.60 kcal/mol which is comparable to binding free energy of reference drug ciprofloxacin (-6.62 kcal/mol) and the binding free energy of title molecule-4DFU protein complex is -2.35 kcal/mol which is comparable to reference drug (-4.95 kcal/mol) as calculated by same docking protocol. The binding pattern of title molecule and binding energy values suggests its high inhibitory potential in comparable to reference drug and thus this study opens up new research platform for further research in imidazole based quinoxaline compounds as biotin carboxylase and antibiotic resistant enzyme aminoglycoside phosphorylase APH(2")IVA inhibitors.

TABLE-16
PREDICTED BINDING FREE ENERGIES (Kcal/mol) OF BEST RANKED 4-STRUCTURE OF TITLE MOLECULE AND REFERENCE DRUG CIPROFLOXACIN WITH PROTEIN 2V59 AND 4DFU EVALUATED FROM ParDock SERVER

Ligands	Best ranked 4-structure	ΔG (Kcal/mol) (2V59)	ΔG (Kcal/mol) (4DFU)
Title molecule	1	-4.60	-2.35
	2	-4.09	-2.16
	3	-3.82	-1.90
	4	-3.74	-1.43
Ciprofloxacin	1	-6.62	-4.95
	2	-6.61	–
	3	-6.51	–
	4	-6.19	–

Conclusion

The imidazole moiety and sulfanyl group containing quinoxaline moiety, novel 2,3-*bis*[(1-methyl-1*H*-imidazole-2-yl)-sulfanyl]quinoxaline have been rationally designed and structure optimization and characterized by IR spectral analysis, ^{1}H, ^{13}C NMR and UV-visible spectral analysis by using suitable theoretical tools. After, a successful optimization of quinoxaline, the aim of computational methods was obtained molecular structure and chemical reactivity descriptors that are not obtained by experimental ways. The theoretically calculated IR spectrum of the compound was analyzed by using DFT/6-311++G(d,p) in the gas phase and mode of vibrations and potential energy distributions (PED) of title molecule was analyse using GaussView 5.0 and VEDA 4.0 program and the vibrational frequencies and infrared intensities shows good agreements with experimental wave numbers given in literature. The solvent effect on ^{1}H, ^{13}C NMR chemical shift of compound analyses and calculated with the help of gauge-including atomic orbital (GIAO) approach and B3LYP/6-311++G(d,p) basis set and the gas phase chemical shift showing good agreement with solvent phase. The solvent effect on absorption maximum (λ_{max}), transition energy (E) and oscillator strength (f) and UV-visible spectrum of the molecule have been studied by time dependent density functional theory (TD-DFT) method using TD-DFT/6-311++G(d,p) basis set in the gas phase and solvent water, DMSO, chloroform using IEF-PCM model. The gas phase UV-visible spectrum of title molecule shows a highest λ_{max} at 425.44 nm corresponding to H-1→L (45 %). The HOMO, LUMO and HOMO-LUMO energy gap (highest E_{gap} = 3.69630 eV in water) and DFT based reactivity descriptors of the title molecule were analyzed by using DFT/B3LYP/6-311++G(d,p) basis set in gas phase and solvent phase (water, DMSO and chloroform) using IEF-PCM model and correlate. The chemical reactivity descriptors such as electronegativity (highest χ = 4.95398 eV in water) chemical potential (highest μ = -4.95398 eV in water) electrophilicity index (highest ω = 6.63958 in water) high values indicate that the title molecule is interacting more efficiently in the biological environment. The higher value of chemical hardness (highest η = 1.84815 eV in water), which is measure of biological membrane penetrating capacity of the title molecule. The Fukui function, MPA, MESP can be used for interpreting and predicting the reactive behaviour of wide variety of chemical systems and also their results are supporting each other about electrophilic and nucleophilic nature of title molecule. The most electrophilic attacking site is C1 > C35 and nucleophilic attacking site is S15 > S16 of the title molecule calculated using DFT/6-311++G(d,p) method in gas phase. The DFT/6-311++G(d,p) basis set in the gas phase calculated dipole moment (μ), polarizability (α), anisotropy of polarizability ($\Delta\alpha$) and first order hyperpolarizability (β_{tot}) results indicates that the title molecule has a reasonable good non-linear optical (NLO) material because the dipole moment, polarizability and hyperpolarizability of the title molecule 3 times, 39 times and 717 times greater than the urea molecule, respectively. The physico-chemical and ADMET parameters for the title molecule has shown that this molecule have good oral drug like properties and could be developed as oral drug candidates and shows good agreement with reference drug ciprofloxacin. Furthermore, the title molecule not shown the any violations with respect to Lipinski "rule of five", CMC like rule, WDI like rule and lead like rule and shows good bioavailability and drug likeness score. Furthermore, the gastrointestinal absorption, skin permeability, caco2 and plasma protein binding percentage of title molecule are highest and show good agreements with reference drug ciprofloxacin. The

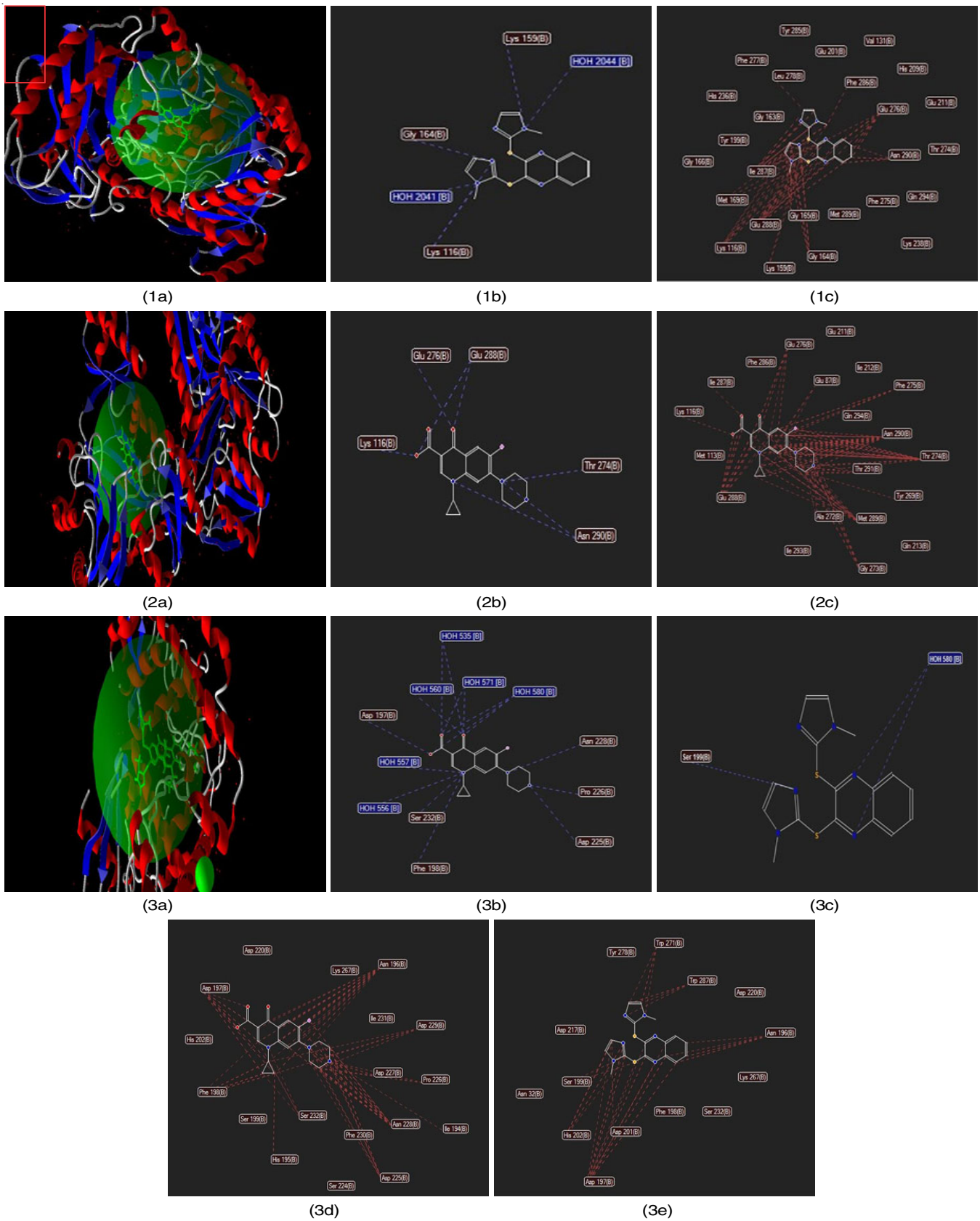

Fig. 15. Molecular docking of the title molecule and reference drug ciprofloxacin with the enzymes of *E. coli* (PDB ID: 2V59) and *Enterococcus casseliflavus* (PDB ID: 4DFU): 1a) and 2a) 3D confirmation of active site and energy map of title molecule and ciprofloxacin binding in biotin carboxylase, 1b), 2b) and 1c), 2c) 2D scheme showing the hydrogen bond and steric interactions of title molecule and ciprofloxacin with amino acids residues of biotin carboxylase enzyme, 3a) 3D confirmation of active site and energy map of title molecule and ciprofloxacin binding in antibiotic resistant enzyme aminoglycoside phosphorylase APH(2")IVA, 3b) and 3c) 2D scheme showing hydrogen bonding of ciprofloxacin and title molecule, and 3d) and 3e) scheme showing steric interactions of ciprofloxacin and title molecule, respectively

toxicity profiles of the title molecule are Ames test positive (mutagen) and the results not shows carcinogenicity in mice and rat, the title molecule possess a high safety profile and also indicated the selectivity of the antimicrobial action. The molecular docking was performed to mockup the interaction between the title molecule and active site of biotin carboxylase of *E. coli* K12 strain (PDB ID: 2v59) and antibiotics resistant aminoglycoside phosphorylase APH(2")IVA of *Enterococcus casseliflavus* (PDB ID: 4DFU) at molecular level, to predict the probable mechanism of action of the title molecule exhibit inhibitory activity against biotin carboxylase enzyme and antibiotics resistant aminoglycoside phosphorylase APH(2")IVA enzyme and shows good agreement with reference drug ciprofloxacin. The rationally designed novel title molecule is very attractive antimicrobial leads and can serve as an excellent scaffold for the further study. Therefore, it is hoped that the results of present study will encourage and support the researchers to discover and synthesize new quinoxaline derivatives.

ACKNOWLEDGEMENTS

The authors are thankful to The Head, Department of Chemistry, University of Lucknow, Lucknow, India for providing central facility for computational research (CFCR).

CONFLICT OF INTEREST

The authors declare that there is no conflict of interests regarding the publication of this article.

REFERENCES

1. H.W. Boucher, G.H. Talbot, J.S. Bradley, J.E. Edwards, D. Gilbert, L.B. Rice, M. Scheld, B. Spellberg and J. Bartlett, *Clin. Infect. Dis.*, **48**, 1 (2009); https://doi.org/10.1086/595011
2. G. Taubes, *Science*, **321**, 356 (2008); https://doi.org/10.1126/science.321.5887.356
3. A.Y. Peleg and D.C. Hooper, *N. Engl. J. Med.*, **362**, 1804 (2010); https://doi.org/10.1056/NEJMra0904124
4. R.J. Heath, S.W. White and C.O. Rock, *Prog. Lipid Res.*, **40**, 467 (2001); https://doi.org/10.1016/S0163-7827(01)00012-1
5. J.W. Capbelll and J.E. Jr Cronan, *Annu. Rev. Microbiol.*, **55**, 305 (2001).
6. Y.M. Zhang, S.W. White and C.O. Rock, *J. Biol. Chem.*, **281**, 17541 (2006); https://doi.org/10.1074/jbc.R600004200
7. A. Kucers, S. Crowe, M.L. Grayson and J. Hoy, The Use of Antibiotics: A Clinical Review of Antibacterial, Antifungal, and Antiviral Drugs, Butterworth Heinemann: Oxford, edn 5, pp. 452-457 (1997).
8. J. Davies and G. Wright, *Trends Microbiol.*, **5**, 234 (1997); https://doi.org/10.1016/S0966-842X(97)01033-0
9. T.C. Broussard, A.E. Price, S.M. Laborde and G.L. Waldrop, *Biochemistry*, **52**, 3346 (2013); https://doi.org/10.1021/bi4000707
10. A.K. Patidar, M. Jeyakandan, A.K. Mobiya and G. Selvam, *Int. J. PharmTech Res*., 3, 386 (2011).
11. S. Au, J. Schacht and N. Weiner, *Biomembranes*, **862**, 205 (1986); https://doi.org/10.1016/0005-2736(86)90484-0
12. S.T. Nguyen, J.D. Williams, M.M. Butler, X. Ding, D.M. Mills, T.F. Tashjian, R.G. Panchal, S.K. Weir, C. Moon, H.O. Kim, J.A. Marsden, N.P. Peet and T.L. Bowlin, *Bioorg. Med. Chem. Lett.*, **24**, 3366 (2014); https://doi.org/10.1016/j.bmcl.2014.05.094
13. R. Musiol, M. Serda, S.P. Hensel-Bielowka and J. Polanski, *J. Curr. Med. Chem.*, **17**, 1960 (2010); https://doi.org/10.2174/092986710791163966
14. J.P. Kleim, R. Bender, U.M. Billhardt, C. Meichsner, G. Riess, M. Rosner, I. Winkler and A. Paessens, *Antimicrob. Agents Chemother.*, **37**, 1659 (1993); https://doi.org/10.1128/AAC.37.8.1659
15. M. Suresh, P. Lavanya, D. Sudhakar, K. Vasu and C.V. Rao, *J. Chem. Pharm. Res.*, **2**, 497 (2010).
16. V.K. Tandon, D.B. Yadav, H.K. Maurya, A.K. Chaturvedi and P.K. Shukla, *Bioorg. Med. Chem.*, **14**, 6120 (2006); https://doi.org/10.1016/j.bmc.2006.04.029.
17. B. Zarranz, A.A. Jaso, I. Aldana and A. Monge, *Bioorg. Med. Chem.*, **11**, 2149 (2003); https://doi.org/10.1016/S0968-0896(03)00119-6.
18. M.M. Badran, A.A. Moneer, H.M. Refaat and A.A. El-Malah, *J. Chin. Chem. Soc.*, **54**, 469 (2007); https://doi.org/10.1002/jccs.200700066.
19. B. Solano, V. Junnotula, A. Marin, R. Villar, A. Burguete, E. Vicente, S. Perez-Silanes, I. Aldana, A. Monge, S. Dutta, U. Sarkar and K.S. Gates, *J. Med. Chem.*, **50**, 5485 (2007); https://doi.org/10.1021/jm0703993.
20. G. Olayiwola, C.A. Obafemi and F.O. Taiwo, *Afr. J. Biotechnol.*, **6**, 777 (2007).
21. A. Wadood, N. Ahmed, L. Shah, A. Ahmad, H. Hassan and S. Shams, *Drug Des. Devel. Ther.*, **1**, 3 (2013).
22. E. Krovat, T. Steindl and T. Langer, *Curr. Comp-Aid. Drug Des.*, **1**, 93 (2005); https://doi.org/10.2174/1573409052952314.
23. V. Alcolea, D. Plano, D.N. Karelia, J.A. Palop, S. Amin, C. Sanmartín and A.K. Sharma, *Eur. J. Med. Chem.*, **113**, 134 (2016); https://doi.org/10.1016/j.ejmech.2016.02.042.
24. M.J. Frisch, G.W. Trucks, H.B. Schlegel, G.E. Scuseria, M.A. Robb, J.R. Cheeseman, G. Scalmani, V. Barone, B. Mennucci, G.A. Petersson, H. Nakatsuji, M. Caricato, X. Li, H.P. Hratchian, A.F. Izmaylov, J. Bloino, G. Zheng, J.L. Sonnenberg, M. Hada, M. Ehara, K. Toyota, R. Fukuda, J. Hasegawa, M. Ishida, T. Nakajima, Y. Honda, O. Kitao, H. Nakai, T. Vreven, J.A. Montgomery Jr., J.E. Peralta, F. Ogliaro, M. Bearpark, J.J. Heyd, E. Brothers, K.N. Kudin, V.N. Staroverov, R. Kobayashi, J. Normand, K. Raghavachari, A. Rendell, J.C. Burant, S.S. Iyengar, J. Tomasi, M. Cossi, N. Rega, J.M. Millam, M. Klene, J.E. Knox, J.B. Cross, V. Bakken, C. Adamo, J. Jaramillo, R. Gomperts, R.E. Stratmann, O. Yazyev, A.J. Austin, R. Cammi, C. Pomelli, J.W. Ochterski, R.L. Martin, K. Morokuma, V.G. Zakrzewski, G.A. Voth, P. Salvador, J.J. Dannenberg, S. Dapprich, A.D. Daniels, Ö. Farkas, J.B. Foresman, J.V. Ortiz, J. Cioslowski and D.J. Fox, Gaussian, Inc., Wallingford CT (2009).
25. K.R. Cousins, *J. Am. Soc.*, **133**, 8388 (2011); https://doi.org/10.1021/ja204075s
26. E. Frich, H. P. Hratchian, R. D. Dennington II, T. A. Keith, John Millam, B. Nielsen, A. J. Holder, J. Hiscocks. Gaussian. Inc. GaussView Version 5.0.8 (2009).
27. M.H. Jamroz, Vibrational Energy Distribution Analysis: VEDA 4 Program, Warsaw, Poland (2004).
28. M.J. Frisch, J.A. Pople and J.S. Binkley, *J. Chem. Phys.*, **80**, 3265 (1984); https://doi.org/10.1063/1.447079
29. R. Ditchfield, *Mol. Phys.*, **27**, 789 (1974); https://doi.org/10.1080/00268977400100711
30. N.M. O'boyle, A.L. Tenderholt and K.M. Langner, *J. Comput. Chem.*, **29**, 839 (2008); https://doi.org/10.1002/jcc.20823
31. A. Kumar, A. Pandey and A. Mishra, *J. Biol. Chem. Res.*, **36**, 1 (2019).
32. A.D. Bochevarov, E. Harder, T.F. Hughes, J.R. Greenwood, D.A. Braden, D.M. Philipp, D. Rinaldo, M.D. Halls, J. Zhang and R.A. Friesner, *Int. J. Quant. Chem*., **113**, 2110 (2013); https://doi.org/10.1002/qua.24481
33. A. Pandey, A. Kumar and A. Mishra, *J. Biol. Chem. Res.*, **36**, 102 (2019).
34. A. Pandey, A. Kumar and A. Mishra, *Int. J. Sci. Res. Rev.*, **8**, 2087 (2019).
35. http://www.molinspiration.com.
36. http://www.acdlabs.com.
37. http://www.swissadme.ch/index.php.
38. http://preadmet.bmdrc.kr.
39. www.molsoft.com/cgi-bin/msearch.cgi.
40. http://tox.charite.de/protox_II/.
41. http://www.rcsb.org/pdb.
42. R. Thomsen and M.H. Christensen, *J. Med. Chem.*, **49**, 3315 (2006); https://doi.org/10.1021/jm051197e
43. A. Gupta, P. Sharma and B. Jayaram, *Protein Pept. Lett.*, **14**, 632 (2007); https://doi.org/10.2174/092986607781483831
44. I. Fleming, Frontier Orbitals and Organic Chemical Reactions, Wiley: London (1976).

45. A.M. Asiri, M. Karabacak, M. Kurt and K.A. Alamry, *Spectrochim. Acta A Mol. Biomol. Spectrosc.*, **82**, 444 (2011); https://doi.org/10.1016/j.saa.2011.07.076
46. B. Kosar and C. Albayrak, *Spectrochim. Acta A Mol. Biomol. Spectrosc.*, **78**, 160 (2011); https://doi.org/10.1016/j.saa.2010.09.016
47. Y.N. Mabkhot, F.D. Aldawsari, S.S. Al-Showiman, A. Barakat, S.M. Soliman, M.I. Choudhary, S. Yousuf, M.S. Mubarak and T.B. Hadda, *Chem. Cent. J.*, **9**, 24 (2015); https://doi.org/10.1186/s13065-015-0100-9
48. S. Suganthi, P. Balu, V. Sathyanarayanamoorthi, V. Kannappan, M. G. Mohamed Kamil, R. Kumar, *J. Mol. Struct*., **1108**, 1 (2016); https://doi.org/10.1016/j.molstruc.2015.11.069
49. R.G. Parr, L.V. Szentpaly and S. Liu, *J. Am. Chem. Soc.*, **121**, 1922 (1999); https://doi.org/10.1021/ja983494x
50. O. Tamer, B. Sariboga and I. Uçar, *Struct. Chem.*, **23**, 659 (2012); https://doi.org/10.1007/s11224-011-9910-0
51. E. Scrocco and J. Tomasi, *Adv. Quantum Chem.*, **11**, 115 (1978); https://doi.org/10.1016/S0065-3276(08)60236-1
52. F.J. Luque, J.M. Lopez and M. Orozco, *Theor. Chem. Acc.*, **103**, 343 (2000); https://doi.org/10.1007/s002149900013
53. G. Schneider, Prediction of Drug-Like Properties, In: Madame Curie Bioscience Database, Landes Bioscience: Austin (TX) (2000-2013).
54. J.C. Adams, M.J. Keiser, L. Basuino, H.F. Chambers, D.-S. Lee, O.G. Wiest and P.C. Babbitt *PLoS Comput. Biol*., **5**, e1000474 (2009) https://doi.org/10.1371/journal.pcbi.1000474
55. J.M. Seminario, Molecular Electrostatic Potentials, Concepts and Applications, Elsevier: Amsterdam (1996).
56. P.W. Ayers and R.G. Parr, *J. Am. Chem. Soc.*, **122**, 2010 (2000); https://doi.org/10.1021/ja9924039
57. R.G. Parr and W.J. Yang, *Am. Chem. Soc.*, **106**, 4049 (1984); https://doi.org/10.1021/ja00326a036
58. W. Yang and W.J.J. Mortier, *J. Am. Chem. Soc.*, **108**, 5708 (1986); https://doi.org/10.1021/ja00279a008
59. R.K. Roy, S. Krishnamurti, P. Geerlings and S. Pal, *J. Phys. Chem. A*, **102**, 3746 (1998); https://doi.org/10.1021/jp973450v
60. P.K. Chattaraj, B. Maiti and U. Sarkar, *J. Phys. Chem. A*, **107**, 4973 (2003); https://doi.org/10.1021/jp034707u
61. M. Govindarajan, M. Karabacak, S. Periandy and D. Tanuja, *Spectrochim. Acta A Mol. Biomol. Spectrosc.*, **97**, 231 (2012); https://doi.org/10.1016/j.saa.2012.06.014
62. R.S. Mulliken, *J. Chem. Phys.*, **23**, 1833 (1955); https://doi.org/10.1063/1.1740588
63. E.R. Davidson and S. Chakravorty, *Theor. Chim. Acta*, **83**, 319 (1992); https://doi.org/10.1007/BF01113058
64. M.D. Segall, C.J. Pickard, R. Shah and M.C. Payne, *Mol. Phys.*, **89**, 571 (1996); https://doi.org/10.1080/002689796173912
65. R.M. Silverstein, G.C. Basseler and C. Morill, Spectroscopic Identification of Organic Compounds, Wiley, New York (1981).
66. R. Shunmugam and D.N. Sathyanarayana, *Spectrochim. Acta A Mol.. Spectrosc.*, **40**, 757 (1984); https://doi.org/10.1016/0584-8539(84)80100-2
67. A.R. Prabhakaran and S. Mohan, *Indian J. Phys.*, **63B**, 468 (1989).
68. R.M. Silverstein, F.X. Webster and D. Kiemle, Spectrometric Identification of Organic Compounds, John Wiley & Sons Inc., edn 2 (2005).
69. M. Karabacak, C. Karaca, A. Atac, M. Eskici, A. Karanfil and E. Kose, *Spectrochim. Acta A Mol. Biomol. Spectrosc.*, **97**, 556 (2012); https://doi.org/10.1016/j.saa.2012.05.087
70. D. Sajan, H. Joe, V.S. Jayakumar and J. Zaleski, *J. Mol. Struct.*, **785**, 43 (2006); https://doi.org/10.1016/j.molstruc.2005.09.041
71. V.M. Geskin, C. Lambert and J.-L. Brédas, *J. Am. Chem. Soc.*, **125**, 15651 (2003); https://doi.org/10.1021/ja035862p
72. R. Zhang, B. Du, G. Sun and Y. Sun, *Spectrochim. Acta A Mol. Biomol. Spectrosc.*, **75**, 1115 (2010); https://doi.org/10.1016/j.saa.2009.12.067
73. A. Verma, *Asian Pac. J. Trop. Biomed.*, **2**, S1735 (2012); https://doi.org/10.1016/S2221-1691(12)60486-9
74. C.A. Lipinski, F. Lombardo, B.W. Dominy and P.J. Feeney, *Adv. Drug Deliv. Rev.*, **46**, 3 (2001); https://doi.org/10.1016/S0169-409X(00)00129-0
75. P. Ertl, B. Rohde and P. Selzer, *J. Med. Chem.*, **43**, 3714 (2000); https://doi.org/10.1021/jm000942e
76. N. Roy and R.U. Kadam, *Indian J. Pharm. Sci.*, **69**, 609 (2007); https://doi.org/10.4103/0250-474X.38464
77. A.K. Ghose, T. Herbertz, R.L. Hudkins, B.D. Dorsey and J.P. Mallamo, *ACS Chem. Neurosci.*, **3**, 50 (2012); https://doi.org/10.1021/cn200100h
78. D.E. Pires, T.L. Blundell and D.B. Ascher, *J. Med. Chem.*, **58**, 4066 (2015); https://doi.org/10.1021/acs.jmedchem.5b00104
79. A. Daina and V. Zoete, *ChemMedChem*, **11**, 1117 (2016); https://doi.org/10.1002/cmdc.201600182
80. F. Yamashita and M. Hashida, *Drug. Metab. Pharm.*, **19**, 327 (2004); https://doi.org/10.2133/dmpk.19.327
81. F.J. Azeredo, F.T. Uchoa and T.D. Costa, *Rev. Bras. Farm.*, **90**, 321 (2009).
82. B.N. Ames, E.G. Gurney, J.A. Miller and H. Bartsch, *Proc. Natl. Acad. Sci. USA*, **69**, 3128 (1972); https://doi.org/10.1073/pnas.69.11.3128
83. M.N. Drwal, P. Banerjee, M. Dunkel, M.R. Wettig and R. Preissner, *Nucleic Acids Res.*, **42(W1)**, W53 (2014); https://doi.org/10.1093/nar/gku401
84. F. Ntie-Kang, L.L. Lifongo, J.A. Mbah, L.C. Owono Owono, E. Megnassan, L.M. Mbaze, P.N. Judson, W. Sippl and S.M.N. Efange, *In Silico Pharmacol.*, **1**, 12 (2013); https://doi.org/10.1186/2193-9616-1-12
85. J.R. Miller, S. Dunham, I. Mochalkin, C. Banotai, M. Bowman, S. Buist, B. Dunkle, D. Hanna, H.J. Harwood, M.D. Huband, A. Karnovsky, M. Kuhn, C. Limberakis, J.Y. Liu, S. Mehrens, W.T. Mueller, L. Narasimhan, A. Ogden, J. Ohren, J.V.N.V. Prasad, J.A. Shelly, L. Skerlos, M. Sulavik, V.H. Thomas, S. Vander Roest, L.A. Wang, Z. Wang, A. Whitton, T. Zhu and C.K. Stover, *Proc. Natl. Acad. Sci. USA*, **106**, 1737 (2009); https://doi.org/10.1073/pnas.0811275106
86. S. Velankar, P. McNeil, V. Mittard-Runte, A. Suarez, D. Barrell, R. Apweiler and K. Henrick, *Nucleic Acids Res.*, **33**, D262 (2004); https://doi.org/10.1093/nar/gki058